DESTRUCTION OF INVARIANT CURVES IN THE RESTRICTED CIRCULAR PLANAR THREE BODY PROBLEM USING COMPARISON OF ACTION

JOSEPH GALANTE AND VADIM KALOSHIN

ABSTRACT. The classical principle of least action says that orbits of mechanical systems extremize action; an important subclass are those orbits that minimize action. In this paper, we utilize this principle along with Aubry-Mather theory to construct instability regions for a certain three body problem. We consider a Sun-Jupiter-Comet system and under some simplifying assumptions, we show the existence of instabilities for orbit of the comet. In particular we show that a comet which starts close to orbit of an ellipse of eccentricity to $e = 0.66$ (fig **??**) can increase in eccentricity up $e = 0.96$. Such an initial orbit is well within the range of our solar system. This might give an indication of why most objects rotating around the Sun in our solar system have relatively low eccentricity. A more technical formulation is as follows.

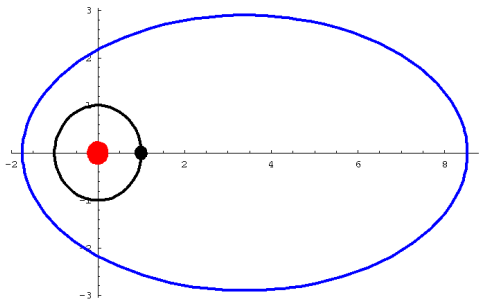

FIGURE 1. Ellipse of Eccentricity $e = 0.66$.
labelrange-of-motion

We consider the so called restricted circular planar three body problem (RCP3BP) which has a conserved quantity called a Jacobi constant J. Fixing J specifies the Hill regions, the regions of allowable motion for the comet [AKN]. We pick J so that there are three disjoint Hill regions; the outer Hill region is unbounded and bounds the comet away from collisions with Jupiter. In this paper, we develop general methods for construction of (Birkhoff) regions of instability for RCP3BP in the outer Hill region corresponding to eccentricities $e^*(\mu, J) \leq e \leq e_{max}(\mu, J)$. The upper bound e_{max} arises from degeneracies in Delauney variables for nearly parabolic motions. We transcend this limitation in [GK2] and prove the existence of an ejection orbit.

We would like to point out that existence of ejection orbits and Chazy instabilities for RCP3BP was established by Llibre and Simo [LS]. We estimate their $e^*(0.001, 1.8) \approx 0.985$, however their motions belong to a horseshoe, while ours have a fairly different nature. We fix plausible values for the Solar System, and use $J = 1.8$ to carry out the details. The main result is the following.

Theorem 0.1. *Consider the restricted circular planar three body problem with Sun-Jupiter mass ratio μ. Fix a Jacobi Constant J that produces three disjoint Hill regions and consider dynamics in the outer Hill region. Then there exist trajectories of a comet with initial eccentricity $e^* = e(\mu, J)$ that increases to eccentricity $e_{max}(\mu, J)$. For example if $\mu = 10^{-3}$ and $J = 1.8$, then $e^* \leq 0.66$ and $e_{max} \geq 0.96$.*

The primary tools for this result will be the applicability of Aubry-Mather theory to the restricted circular planar three body problem, and the implementation of rigorous numerical integration. We stress that trajectories are **not** constructed by means of numerical integration. After a mathematical framework is developed, we derive a list of inequalities. To have an explicit value of e^*, we use a computer to verify the range of validity of the inequalities, which are of two types: analytic and dynamic. Analytic inequalities do not make use to integration of the equations of motion. Dynamical inequalities do involve integration, but only over short periods of time. We use software which can handle both types of inequalities in a mathematically rigorous way.

1. Introduction

We consider the restricted circular planar three body problem (RCP3BP) with two massive primaries, which we call the Sun and Jupiter, that perform uniform circular motion about their center of mass. (See fig. 2) The system is normalized to mass one so the Sun has mass $1-\mu$ and Jupiter mass μ. We further normalize so that Jupiter rotates with period 2π, and the distance from the Sun to Jupiter is constant and also normalized to one. Our goal is to understand the behavior of the massless comet whose position in polar coordinates is denoted (r, ψ). It is convenient to consider the system in a rotating frame of reference which rotates with unit speed in the same direction as Jupiter. In this system, the Sun and Jupiter are fixed points on a line, say the x-axis. We let $(r, \varphi) = (r, \psi - t)$ denote the motion of the comet in the rotating frame of reference. The motions of the comet can be viewed as the solutions to Hamilton's equations with a Hamiltonian of the form

$$H = H_{2BP} + \Delta H(r, \varphi) := \frac{P_r^2}{2} + \frac{P_\varphi^2}{2r^2} - P_\varphi - \frac{1}{r} + \Delta H(r, \varphi) \tag{1}$$

where ΔH (denoted below) is the perturbation of the associated Sun-Comet two body problem (2BP(SC)) and P_r and P_φ are the momenta variables conjugate to r and φ [CC]. (This system arises by initially considering the planar 3BP where

the comet has mass m, and letting $m \to 0$.) If d_J is the Jupiter-Comet distance

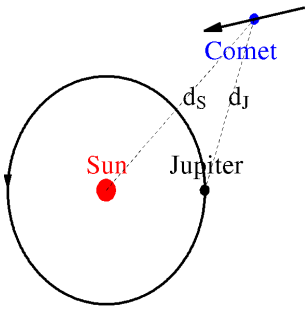

FIGURE 2. Sun-Jupiter-Comet.

and d_S is the Sun-Comet distance, then ΔH can be written

$$d_J(r,\varphi) = (r^2 - 2(1-\mu)r\cos(\varphi) + (1-\mu)^2)^{\frac{1}{2}} \tag{2}$$

$$d_S(r,\varphi) = (r^2 + 2\mu r\cos(\varphi) + \mu^2)^{\frac{1}{2}} \tag{3}$$

$$\Delta H = \frac{1}{r} - \frac{\mu}{d_J} - \frac{1-\mu}{d_S} = \frac{\mu(1-\mu)(1-3\cos(2\varphi))}{2r^3} + O\left(\frac{\mu}{r^4}\right). \tag{4}$$

It turns out the RCP3BP has a conserved quantity known as the *Jacobi constant*.

$$J(r,\varphi,\dot{r},\dot{\varphi}) = \frac{r^2}{2} + \frac{\mu}{d_J} + \frac{1-\mu}{d_S} - \frac{\dot{r}^2 + r^2\dot{\varphi}^2}{2} =: U(r,\varphi) - \frac{\dot{r}^2 + r^2\dot{\varphi}^2}{2}. \tag{5}$$

Let $\mathcal{H}(J_0) = \{(r,\varphi) : \ U \geq J_0\}$ denote the Hill regions associated to the Jacobi constant J_0. These regions are the locations in the (r,φ) plane (shaded regions in figure 3) where the comet is allowed to move. Denote by $\mathcal{H}^{out}(J_0)$ the *outer*

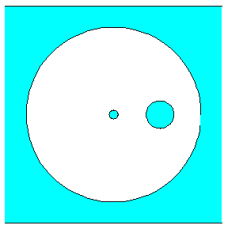

FIGURE 3. Hill Regions.

Hill region which is the noncompact region of allowable motions. It is here that escape may be possible. For $\mu = 10^{-3}$, such a region exists for $J_0 \geq 1.52$. (This value arises by considering the 'zero velocity' curves which are on the boundary of the Hill regions. [AKN]) Examination the equations of motion, reveals they depend only on the variables (r,φ) as well as velocity. Hence the phase space $\mathbb{R}^4$ is foliated by invariant generically 3-dimensional surfaces. Fixing

the Jacobi constant gives dynamics on one of these 3-dimensional surfaces, which we denote

$$\mathcal{S}(J_0) = \{(r, \varphi, \dot{r}, \dot{\varphi}) : J(r, \varphi, \dot{r}, \dot{\varphi}) = J_0\}. \tag{6}$$

Denote by RCP3BP(μ,J_0) the RCP3BP with Sun-Jupiter mass ratio μ and dynamics restricted to $\mathcal{S}(J_0)$.

Lemma 1.1. *If $(r, \varphi, \dot{r}, \dot{\varphi})(0) \in \mathcal{S}(J_0)$, then $(r(t), \varphi(t)) \in \mathcal{H}(J_0)$.*

Lemma 1.2. *Trajectories in $\mathcal{H}^{out}(J_0)$ satisfy $\frac{J_0^2}{2} - 8\mu \leq r(t)$ for all t.*

As the position of Jupiter is at radius $1 - \mu$, then this lemma implies that if the comet is in the outer Hill region, it will remain bounded away from collisions with the Sun and Jupiter for all time by at least 0.145.

For small μ and away from collisions, RCP3BP is nearly integrable and can be approximated with the 2BP(SC) (ie $\mu = 0$). Elliptic motions of a 2BP have two special points where the radial velocity $\dot{r}$ of the comet is zero. The *perihelion* is the closest point to the Sun, denoted r^{perih}, and the *apohelion* is the farthest point from the Sun, denoted r^{apoh}. Define the *osculating (or instantaneous) eccentricity* $e(t)$ for the RCP3BP to be the eccentricity of the comet in the unperturbed 2BP(SC) system with initial conditions taken to be those of comet in the RCP3BP at time t.

1.1. **The Main Theorem.** It is natural to think of the coordinates on $\mathcal{S}(J_0)$ as (e, φ, t). We say that a surface $\mathcal{T}^2 \subset \mathcal{S}(J_0)$ is an *invariant 2-torus of RCP3BP* (μ, J_0) if there is a smooth invariant surface given by the graph $\{e(\varphi, t) : (\varphi, t) \in \mathbb{T}^2\}$ of a smooth function $e\colon T^2 \to \mathbb{R}_+$. In particular, the existence such a surface would separate the energy surface $\mathcal{S}(J_0)$. When $\mu = 0$ (i.e. when there is no perturbation), the problem reduces to the 2BP(SC) system and every such surface is defined by $\{e = e_0 \geq 0\}$. Bounded motions coorespond to $e_0 \in [0, 1)$. In general, for $\mu > 0$ and for e small and bounded away from 1, many of these invariant 2-tori survive due to KAM [dLll]. One of the corollaries of our results is the existence of a region free of invariant 2-tori. Celleti and Chierchia gave a computer assisted proof using $\mu \approx 10^{-3}$ and $J_0 \approx 1.76$ which could be adapted to show that near $e = 0.3$ there is an invariant 2-torus $\mathcal{T}^2$ separating $\mathcal{S}(J_0)$ into a compact "Below $\mathcal{T}^2$" component and a noncompact "Above $\mathcal{T}^2$" component [CC][1]. We present the method for a specific value of $J_0 = 1.8$, however the method works for any $J_0 \geq 1.52$. [2]

We now restate our main theorem.

[1]Personal Communication

[2]Values $\sqrt{2} \leq J_0 \leq 1.52$ require substantial additional work. For J_0 near or less than $\sqrt{2}$ collisions with Jupiter are hard to exclude.

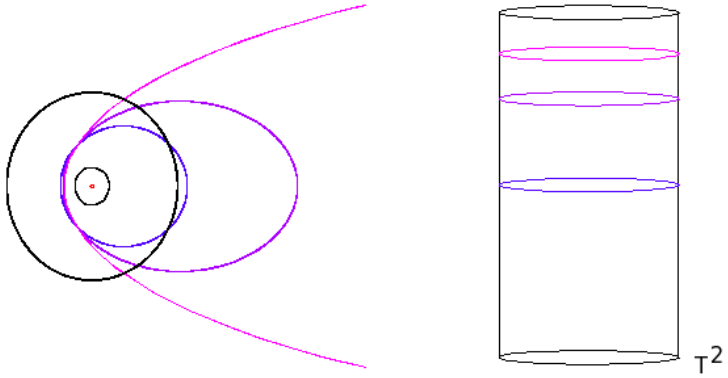

FIGURE 4. Various eccentricity orbits of the 2BP in the plane and on the (φ, t, e) cylinder.

Theorem 1.3. *Consider the restricted circular planar three body problem with Sun-Jupiter mass ratio μ. Fix a Jacobi Constant J that produces three disjoint Hill regions and consider dynamics in the outer Hill region. Then there exists $e^* = e^*(\mu, J_0)$ and $e_{max} = e_{max}(\mu, J_0)$ such that there are no invariant 2-tori crossing the region $e^* \leq e \leq e_{max}$. For example $e(0.001, 1.8) \leq 0.66$ and $e_{max}(0.001, 1.8) \geq 0.96$.*

Later we show that dynamics of RCP3BP(μ, J) in the outer Hill region can be reduced to the study of an exact area preserving twist map (EAPT). Then one way to rephrase Theorem 1.3 is that there exists a *Birkhoff region of instability* in a certain region.

2. Action Comparison Method

"Nature is thrifty in all its actions". - Maupertuis [D]

In this chapter we outline a method for destroying invariant curves based on the method of action comparison.

2.1. **Action-Minimization.** The motions of the comet also satisfy the Euler-Lagrange (EL) equations with Lagrangian

$$L = \frac{v^2}{2} + \frac{1}{r} - \Delta H(r, \varphi) := \frac{\dot{r}^2}{2} + \frac{r^2(\dot{\varphi} + 1)^2}{2} + \frac{1}{r} - \Delta H(r, \varphi) \tag{7}$$

and locally minimize action.

Notice that $L\colon \mathbb{R}^2 \times \mathbb{R}^2 \times \mathbb{T} \to \mathbb{R}$, $L(q, \dot{q}, t)$ given by (7) is a smooth C^r $(r \geq 2)$ positive definite Lagrangian away from Jupiter and the Sun, eg in $\mathcal{H}^{out}(1.8)$. Let $(q_0, t_0), (q_1, t_1) \in \mathbb{R}^2 \times \mathbb{R}$. *Action* along an absolutely continuous curve

$\gamma\colon [t_0, t_1] \to \mathbb{R}^2$ is defined to be

$$A(\gamma) = \int_{t_0}^{t_1} L(\gamma(t), \dot{\gamma}(t), t)dt. \tag{8}$$

We say that a curve $\gamma\colon [t_0, t_1] \to \mathbb{R}^2$ is *action-minimizing* if

$$A(\gamma) = \min_{\gamma\colon [t_0,t_1]\to\mathbb{R}^2 : \gamma(t_0)=q_0, \gamma(t_1)=q_1} A(\gamma) \tag{9}$$

where minimum is taken over all absolutely continuous curves connecting q_0 to q_1. We also say that a curve $\gamma\colon \mathbb{R} \to \mathbb{R}^2$ is *globally action-minimizing* if it is action minimizing on every time interval $[t_0, t_1]$. From the applicability of Aubry–Mather theory it follows that

Lemma 2.1. *If $\mathcal{T}^2$ is an invariant 2-torus of RCP3BP, then every trajectory inside of $\mathcal{T}^2$ is globally action-minimizing.*

We shall prove this result in a later section under the constraint that $e \leq e_{max}$. However lets consider the utility of the result now. Our goal is to show that certain high eccentricity trajectories are **not** globally action minimizing. If this is so, then they are not contained in invariant 2-tori. The main idea is that passing by Jupiter is cheaper at some times than at others. We will exploit this difference and outline the method using some simplifying assumptions, then in a later section develop the formalism to make the method rigorous.

2.2. **Solar Passages and Perihelion Angles.** Consider a trajectory $(r(t), \varphi(t))$ on $\mathcal{S}(J_0) \cap \mathcal{H}^{out}(J_0)$ such that

(**i**) $r(t_1) = R$ for some time t_1,

(**ii**) the trajectory passes through a perihelion $r^{perih} = r(t^*)$ at some $t^* > t_1$ inside the ball of radius J_0^2 , ie $r^{perih} < J_0^2$. (Recall mathematically $\dot{r} = 0$ at the perihelion, and physically it is the closest point to sun.)

(**iii**) $r(t_2) = R$ for $t_2 > t^*$.

Call such a segment of trajectory $(r(t), \varphi(t))_{t\in[t_1,t_2]}$ an *R–Solar passage*. (fig 5). The *perihelion angle*, denoted φ^{perih}, is the angle the comet makes relative to the position of Jupiter at the perihelion. Let $SP(J_0, R)$ be the set of all R–Solar passages. The following lemma guarentees existence of solar passages.

Lemma 2.2. *Fix $\mu = 0.001$ and Jacobi constant $J_0 \geq 1.52$. Consider a trajectory $\gamma(t) = (r(t), \varphi(t))$ in the outer Hill region such that for some time τ we have that $e(\tau) \geq e^*$. Then there exists an R_{max} so that $\gamma(t)$ has a R–Solar passages for all $r^{perih} < R \leq R_{max}$. Furthermore $\frac{J_0^2}{2} - 8\mu \leq r^{perih} \leq J_0^2$.*

We present a heuristic proof of this lemma for $J_0 = 1.8$. Recall that for $\mu = 0$ we have $\dot{e}(t) \equiv 0$. In the 2BP(SC) for $e \geq 0.45$, trajectories are ellipses with apohelion distance to the origin $r^{apoh} \geq 5$. This indicates that there is a

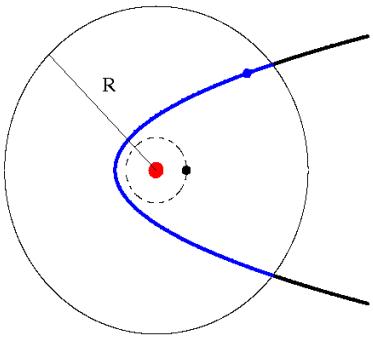

FIGURE 5. An R–Solar passage.

time interval $[t_1, t_2]$ such that $r(t_1) = r(t_2) = R \leq r^{apoh}(e)$, and hence for some $t^* \in [t_1, t_2]$ we have $\dot{r}(t) < 0$ (resp. > 0) for each $t \in (t_1, t^*)$ (resp. (t^*, t_2)). It implies that $r(t^*)$ is a minimum of $r(t)$ on the interval $[t_1, t_2]$. Simple analysis of ΔH shows that $|\Delta H| \leq \frac{2.7\mu}{r^3}$ for $r \geq 1.59$. This implies that $\dot{e}(t) \simeq O(\mu/r^3)$ which is small since $\mu \approx 10^{-3}$, so the shape of the orbit is almost unchanged and hence the minimum, ie the perihelion, will still exist since the comet must turn around eventually. Furthermore there exists an $R_{max} \simeq r^{apoh}(e(\tau))$ so that we have R–Solar passages for all $R \leq R_{max}$. The lower bound on the radius follows from properties of $\mathcal{H}^{out}(1.8)$ and is approached with nearly parabolic motions while the upper bound follows from considering nearly circular motions of the comet.

2.3. **Bad Perihelion Angles.** We will prove that certain R–Solar passages are not action minimizing. It turns out this depends heavily on the perihelion angle during the passage.

Theorem 2.3. *(Bad Angles Theorem) Fix μ and J so that there are three disjoint Hill regions and consider dynamics in the outer Hill region. Then there exists is an interval $[\varphi_-, \varphi_+]$ with $\varphi_\pm = \varphi_\pm(J_0)$, such that if $(r(t), \varphi(t))_{t\in[t_1,t_2]}$ is an R–Solar passage and perihelion angle $\varphi^{perih} \in [\varphi_-, \varphi_+]$, then $(r(t), \varphi(t))_{t\in[t_1,t_2]}$ is not action-minimizing.*

We present the proof of the Bad Angles Theorem in a later section. Combining lemmas 2.2 and 2.1, and theorem 2.3 shows there is an $e^*(\mu, J_0)$ such that there are no invariant 2-tori crossing the region $e \geq e^*(\mu, J_0)$.

Proof of Theorem 1.3. The proof is by contradiction. Suppose there is an invariant 2-torus $\mathcal{T}^2$ of RCP3BP(μ, J_0). Consider the intersection of $\mathcal{T}^2$ with perihelion/apohelion surface $\Sigma = \{\dot{r} = 0\}$. In polar coordinates $\dot{\varphi} < 0$ so trajectories intersect $\{\dot{r} = 0\}$ transversally and thus $\Sigma \cap \mathcal{T}^2$ is diffeomorphic to a compact one-dimensional manifold, i.e. the circle. This implies that for every perihelion angle $\varphi^{perih} = \varphi(t^*)$ there is a trajectory $(r(t), \varphi(t))$ inside $\mathcal{T}^2$ with this

perihelion angle. By Lemma 2.2 there is an R–Solar passage $(r(t), \varphi(t))_{t\in[t_1,t_2]}$ with $t^* \in [t_1, t_2]$ for this trajectory. By Theorem 2.3 this R-Solar passage is **not** action-minimizing, which contradicts lemma 2.1. Thus, there are no invariant 2-tori for RCP3BP(μ, J_0) crossing $e \geq e^*(\mu, J_0)$.

2.4. **Action Decomposition.** In this section we stick to $\mu = 10^{-3}$ and $J_0 = 1.8$ for concreteness. Suppose $\gamma \in SP(1.8, R)$. We decompose γ into (fig 6)

(**i**) γ^- – the part of the curve where r decreases from radius R to radius 5, which we call a $(R, 5)$ *segment*

(**ii**) γ^{in} – a 5–Solar passage

(**iii**) γ^+ – the part of the curve where r increases from radius 5 to radius R, which we call a $(5, R)$ *segment*.

Remark. $5 \approx \frac{3J_0^2}{2}$. For $r \geq 5$ one can show that $|\Delta H| \leq 10^{-5}$. Denote the region $\{r \geq 5\}$ the *outside region* since the comet is practically outside the range of influence of Jupiter. Denote the region $\{r \leq 5\}$ the *kick region* as the comet's orbital parameters are perturbed (or kicked) more in this region.

We denote the action on each of the segments A^-_{out}, A_{in}, and A^+_{out} respectively.

$$A(\gamma) = A^-_{out} + A_{in} + A^+_{out}\,. \tag{10}$$

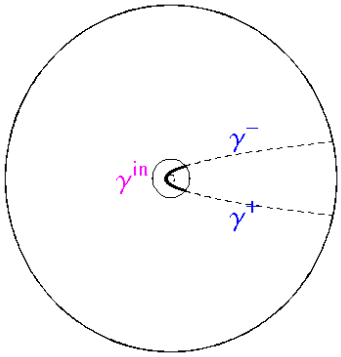

FIGURE 6. Decomposition of γ into smaller arcs.

2.5. **Action Comparison in the Kick Region.** It turns out that A_{in} has fairly sensitive dependence on the perihelion angle. We can explain the difference in actions physically by considering two scenarios. One possibility is that the comet is pulled along behind Jupiter, and gains velocity. This is a so called gravity assist, and when the comet leaves the perihelion, it will be flung further out than before. This case turns out to be action minimizing since the comet is getting a free ride from Jupiter. The other possibility is exactly the reverse. The comet is

slowed down by Jupiter and is pulled more inward, as Jupiter attempts to capture it. Note that Jupiter can never actually capture the comet as a moon since the inner Hill region around Jupiter is separated from the outer region by our choice of Jacobi Constant.

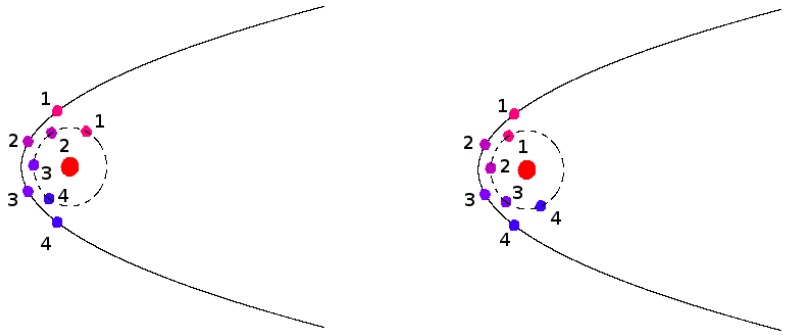

FIGURE 7. Potential Capture and Escape.

According to standard formulas [AKN], it turns out the eccentricity $e = \sqrt{1 - 2P_\varphi^2(J_0 - P_\varphi)}$ where $J_0 = E = -H$ is the energy of the associated Hamiltonian. One can parameterize the 3-dimensional energy surface $\mathcal{S}(J_0)$ with coordinates (r, φ, P_φ). Denote by $SP(J_0, R, P_\varphi)$ the set of all R–Solar passages belonging to $\mathcal{S}(J_0)$ that have initial angular momentum P_φ. Define φ_{max}^{perih} and φ_{min}^{perih} as the angles such that

$$A_{in}(P_\varphi, \varphi_{max}^{perih}) := \max_{\gamma \in SP(J_0,R,P_\varphi)} A(\gamma^{in}) \tag{11}$$

$$A_{in}(P_\varphi, \varphi_{min}^{perih}) := \min_{\gamma \in SP(J_0,R,P_\varphi)} A(\gamma^{in})\,. \tag{12}$$

Remark. It turns out that φ_{min}^{perih} and φ_{min}^{perih} depend slightly on P_φ. We ignore this for now to keep the argument simple.

Lets compute the differences in action and angle as a function of P_φ.

$$\Delta A_{in}^{min}(P_\varphi) = \min_{P_\varphi} \left(A_{in}(P_\varphi, \varphi_{max}^{perih}) - A_{in}(P_\varphi, \varphi_{min}^{perih}) \right) \tag{13}$$

$$\Delta\varphi = \varphi_{max}^{perih} - \varphi_{min}^{perih}\,. \tag{14}$$

To get a feel for these quantities we pick $R = 26$ and $P_\varphi = 1.8$. A computer can then compute $\Delta A_{in}^{min} \approx 0.0163237$ and $\Delta\varphi \approx 1.076$.

Plotted (fig 8) is φ^{perih} vs. the corresponding action of the curve for the particular set of 26–Solar passages corresponding to parabolic motion ($P_\varphi = 1.8$).

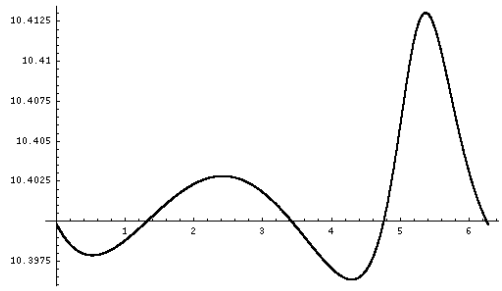

FIGURE 8. Action Difference for nearly parabolic motions.

2.6. **Heuristic Outside Region Action Comparsion.** We now describe a procedure to construct γ_{test}, a new curve with smaller action than γ, ie $A(\gamma_{test}) < A(\gamma)$. Doing this will complete the Bad Angles Theorem since we can take a neighborhood of φ^{perih}_{max} for the interval of angles specified in the theorem. For $r \geq 5$, $|\Delta H| \leq 10^{-5}$, so the perturbation term is neglegibly small away from the Sun and it is not too bad to **approximate the RCP3BP by the 2BP(SC)** for the $(R, 5)$ segment and the $(5, R)$ segments. Doing so allows us to be explicit and compute the action without computer assistance. The approximations will be made rigorous later.

Heuristically if the comet starts at $R = 26$ and has $\varphi^{perih} = \varphi^{perih}_{max}$, then by modifying the velocity of the $(26, 5)$ segment, the comet can slow down enough so that Jupiter will move from a position where the action is maximized to a position where action is minimized. The comet can then speed very slightly during the $(5, 26)$ segment to arrive at $R = 26$ at the same time as in the original case.

Note that it takes a finite amount of time ΔT for the angle of Jupiter relative to the comet to change by $\Delta\varphi$. In nonrotating coordinates Jupiter moves with unit speed, and for $r \geq 5$ the comet's angle remains nearly constant since $\dot{\psi} = \frac{P_\varphi}{r^2}$. (In rotating coordinates, Jupiter is fixed and the comet is moving with almost unit speed.) Hence $\Delta T \approx \Delta\varphi$. By Kepler's Second Law, for $r \geq 5$ the comet moves slower the further away it is from the Sun. We denote the amount of time the comet spends in the $(26, 5)$ segment by T_{out}. (To keep the argument simple, assume by symmetry, this also the time spent in the $(5, 26)$ segment.) A very small change in velocity will change the amount of time to reach the perihelion considerably. Let

$$\lambda_\pm = \frac{T_{out}}{T_{out} \mp \Delta\varphi} \approx \frac{T_{out}}{T_{out} \mp \Delta T}\,. \tag{15}$$

Suppose there exists an invariant 2-torus. Then there are trajectories on it which have all possible perihelion angles. Suppose $\gamma \in SP(1.8, 26)$ is such that the

perihelion angle is φ_{max}^{perih} and $\gamma^{in} \in SP(1.8, 5)$ **maximizes** action over all 5–Solar passages. Consider a new curve γ_{test} where

(**i**) the velocity of the $(26, 5)$ segment is $\dot{\gamma}_{test}^{-} = \lambda_- \cdot \dot{\gamma}^-$

(**ii**) γ_{test}^{in} is a 5–Solar passage which minimizes action over all 5–Solar passages

(**iii**) the velocity of the $(5, 26)$ segment is $\dot{\gamma}_{test}^{+} = \lambda_+ \cdot \dot{\gamma}^+$.

Corollary 2.4. *Suppose $\gamma \in SP(1.8, 26)$ maximizes action during its 5–Solar passage with perihelion angle φ_{max}^{perih}, and γ_{test} is constructed above with perihelion angle φ_{min}^{perih}. If $A(\gamma) - A(\gamma_{test}) > 0$, then γ is not a global action minimizer. Furthermore, there are no global action minimizers in $SP(1.8, R)$, $R \geq 26$.*

Lets calculate the difference in actions between γ and γ_{test}, starting with the action of the rescaled $(26, 5)$ segment γ_{test}^{-}. The Hamiltonian of the 2BP(SC) approximation for parabolic motion gives $\frac{v^2}{2} = \frac{P_r^2}{2} + \frac{P_\varphi^2}{2r^2} = \frac{1}{r}$, where $v = \dot{\gamma}$ is the velocity of γ.

$$A(\gamma_{test}^{-}) = \int_{t(5)\cdot\lambda_-}^{t(26)\cdot\lambda_-} (\frac{\lambda_-^2 v^2}{2} + \frac{1}{r})(\frac{t}{\lambda_-})\, dt \tag{16}$$

$$= \int_{t(5)}^{t(26)} \lambda_-(\lambda_-^2(\frac{1}{r}) + \frac{1}{r})(u)\, du \tag{17}$$

$$= \int_5^{26} \frac{\lambda_-^3 + \lambda_-}{r\dot{r}} dr \tag{18}$$

$$= \int_5^{26} \frac{\lambda_-^3 + \lambda_-}{\sqrt{2r - 1.8^2}}\, dr\,. \tag{19}$$

Remarks. The last line comes from solving $H_{2BP}(r, \varphi, \dot{r}, 1.8) = 1.8$ for $\dot{r}$, as this corresponds to parabolic motion. The limits of integration change since we must start and end at the same place with respect to (r, φ) in the scaled and unscaled cases. By symmetry from the 2BP(SC) approximation, the $(5, R)$ segment γ_{test}^{+} will be the same computation only using λ_+. The unscaled trajectories γ^+ and γ^- will be same computation, only using $\lambda = 1$.

Consider the following formulas relating time and radius for 2BP parabolic motions.

Lemma 2.5. *For parabolic motions in the 2BP,*

$$r(t) = \frac{1}{2}\left(3t + \sqrt{J_0^6 + 9t^2}\right)^{2/3} + \frac{J_0^4}{2\left(3t + \sqrt{J_0^6 + 9t^2}\right)^{2/3}} - \frac{J_0^2}{2} \tag{20}$$

$$t(r) = \frac{1}{3}\sqrt{2r^3 + 3J_0^2 r^2 - J_0^6}\,. \tag{21}$$

Proof. These can be derived from formulas in [AKN] section 2.1.

Using these formulas gives

$$t(5) \approx 7.1413 \tag{22}$$

$$t(26) \approx 68.0594 \tag{23}$$

Then

$$\lambda_- \approx 0.984436 \tag{24}$$

$$\lambda_+ \approx 1.01606 \tag{25}$$

and

$$A(\gamma^-_{test}) \approx 8.49599 \tag{26}$$

$$A(\gamma^+) = A(\gamma^-) \approx 8.76567 \tag{27}$$

$$A(\gamma^+_{test}) \approx 9.0507\,. \tag{28}$$

Now compute the difference in action between the curves γ and γ_{test}.

$$A(\gamma) - A(\gamma_{test}) \geq \Delta A^{min}_{in} + \big(A(\gamma^-) - A(\gamma^-_{test})\big) + \big(A(\gamma^+) - A(\gamma^+_{test})\big) \tag{29}$$

$$\approx 0.000978235 > 0\,. \tag{30}$$

Further analysis indicates that picking any other radius larger than $R = 26$ will also produce a strictly positive result. The reason is that spending more time in the outside region, increases T_{out}, which pushes λ's closer to 1, which makes the differences in action on the $(5, 26)$ and $(26, 5)$ segments smaller, and hence increases the difference in actions between γ and γ_{test}. Hence we conclude that there are no invariant 2-tori corresponding to $R \geq 26$, ie $e \geq 0.88$.

The remainder of this paper is dedicated to making the action comparison method mathematically rigorous.

3. Delauney Variables

For the two body problem there is a natural well defined action angle coordinate system known as Delauney Variables. A derivation of Delauney variables is found in [CC]. In short, they arise by considering the generating function

$$S(r, \varphi, L, G) = \varphi G + \int_{r^{perih}(L,G)}^{r} \sqrt{2\left(\frac{-1}{2L^2} - \frac{P_\varphi^2}{2r^2} + \frac{1}{r} + P_\varphi\right)}\, dr\,. \tag{31}$$

This gives the canonical transformation $\phi_{Del}(r, \varphi, P_r, P_\varphi) = (L, G, \ell, g)$ from polar to Delauney variables where $r^{perih} = L^2\left(1 - \sqrt{1 - \frac{G^2}{L^2}}\right)$ is the perihelion of the 2BP expressed in terms of L, G.

For the 2BP, L^2 is the semi major axis of the ellipse of the orbit, so by Kepler's Third Law, the period $T = 2\pi L^3$. Upon examination of the generating function observe $G = P_\varphi$ is angular momentum. The variable ℓ is the mean anomaly which is $\ell = \pi \mod 2\pi$ at the apohelion, $\ell = 0 \mod 2\pi$ at the perihelion, and in general $(\ell - \ell_0) = \frac{2\pi}{T}t$. Its possible recover radius from Delauney coordinates by noting $r = L^2(1 - e\cos(u))$ where the eccentricity $e = \sqrt{1 - \frac{G^2}{L^2}}$, and u the mean anomaly is given implicitly by $u - e\sin(u) = \ell$. More exposition on anomalies can be found in [AKN] and [CC].

Applying the canonical transformation to H^{2BP}_{Polar} gives

$$H^{2BP}_{Del} = H^{2BP}_{Polar} \circ (\phi_{Del})^{-1} = -\frac{1}{2L^2} - G\,. \tag{32}$$

Note that S satisfies $\det(\frac{\partial^2 S}{\partial(r,\phi)\partial(L,G)}) = \frac{L^3}{P_r} \neq 0$. Hence in general there exists a canonical transformation from polar to Delauney, provided the generating function is well defined [AKN]. Hence where it makes sense, one gets Delauney variables for RCP3BP using the generating function S.

$$H^{3BP}_{Del} = H^{3BP}_{Polar} \circ (\phi_{Del})^{-1} = -\frac{1}{2L^2} - G + \Delta H(L, G, \ell, g) \tag{33}$$

where the perturbation term is converted to Delauney. Unfortunately Delauney variables are is not defined very close to separatrices for the RCP3BP corresponding to nearly parabolic motions. In [GK2] we develop techniques to overcome this limitation.

4. Twisting in Delauney Coordinates

Consider the Poincare section $\Gamma = \{g = 0 \mod 2\pi\}$. Using a computer one can show that $-1.025 < \dot{g} \leq -0.9975$ for $J_0 = 1.8$ and $\mu = 0.001$, and hence Γ is well defined (see appendix for how to derive this estimate). Consider the Poincare return map $\mathcal{F} : \mathcal{S}(J_0) \cap \mathcal{H}(J_0) \cap \Gamma \mapsto \mathcal{S}(J_0) \cap \mathcal{H}(J_0) \cap \Gamma$ defined by

$$\mathcal{F} = \begin{pmatrix} \mathcal{F}_\ell \\ \mathcal{F}_L \end{pmatrix} : \begin{pmatrix} \ell_0 \\ L_0 \end{pmatrix} \mapsto \begin{pmatrix} \ell(t^*, \ell_0, L_0) \\ L(t^*, \ell_0, L_0) \end{pmatrix} \tag{34}$$

where $t^* > 0$ is the first return time to Γ. In this section, we show that in Delauney coordinates, the return map $\mathcal{F}$ is an exact area preserving twist (EAPT) map for $L \leq L_{twist}(\mu, J_0)$. (See [MF], [Ban], [Mo1],and [S] for exposition on EAPT maps). Numerically we find $L_{twist}(0.001, 1.8) \geq 16$.

4.1. **Twisting Conditions.**

Our goal is to develope an explicit condition which can be numerically checked to verify twist. The energy reduction formulas found in the [BK] and [KN] allow us to write an autonomous Hamiltonian system as a time dependent Hamiltonian. Parts of exposition below are taken these sources.

Fix μ and J_0. Suppose the differential of a Hamiltonian $H'_{J_0}(L, G, \ell, g)$ satisfies the following equation:

$$dH'_{J_0}(L, G, \ell, g) = \frac{\left(\frac{\partial H}{\partial \ell}\right)}{\left(\frac{\partial H}{\partial G}\right)} d\ell + \frac{\left(\frac{\partial H}{\partial L}\right)}{\left(\frac{\partial H}{\partial G}\right)} dL + \frac{\left(\frac{\partial H}{\partial g}\right)}{\left(\frac{\partial H}{\partial G}\right)} dg + dG\,. \tag{35}$$

Then trajectories of H'_{J_0} and those of H on the energy surface $S(J_0)$ coincide up to time reparameterization provided that $\frac{\partial H}{\partial G}$ is bounded away from zero. By construction $\frac{\partial H'_{J_0}}{\partial G} \equiv 1$. Consider the implicit function $G = G(L, \ell, g, J_0)$. Noting that $\dot{g} \approx -1$, define a new time periodic Hamiltonian by

$$\tilde{H}_{J_0}(L, \ell, t) = G(L, \ell, g, J_0) - H'_{J_0}(L, \ell, g, G(L, \ell, g, J_0)) \tag{36}$$

where the variable $t = g$. Notice that

$$\frac{\partial}{\partial G}(\tilde{H}_{J_0}(L, \ell, t)) = \left(\frac{\partial G}{\partial G}\right) - \left(\frac{\partial H'_{J_0}}{\partial G}\right)\left(\frac{\partial G}{\partial G}\right) = 1 - 1 \cdot 1 \equiv 0 \tag{37}$$

so it is easy to see that $\tilde{H}_{J_0}$ does not depend on G. Now compute the derviative of $\tilde{H}_{J_0}$ with respect to L.

$$\frac{\partial}{\partial L}\tilde{H}_{J_0}(L, \ell, t) = \frac{\partial G}{\partial L} - \frac{\partial H'_{J_0}}{\partial L} - \left(\frac{\partial H'_{J_0}}{\partial G}\right)\left(\frac{\partial G}{\partial L}\right)\,. \tag{38}$$

But $\frac{\partial H'_{J_0}}{\partial G} \equiv 1$ by construction, so

$$\frac{\partial}{\partial L}\tilde{H}_{J_0}(L, \ell, t) = -\frac{\partial H'_{J_0}}{\partial L} = -\frac{\left(\frac{\partial H(L,\ell,g,G(L,\ell,g,J_0))}{\partial L}\right)}{\left(\frac{\partial H(L,\ell,g,G(L,\ell,g,J_0))}{\partial G}\right)} \tag{39}$$

where the last equality follows by construction of H'_{J_0}. Now look at the second derivative with respect to L.

$$\begin{aligned}
\frac{\partial}{\partial L}\left(\frac{\partial \tilde{H}_{J_0}(L, \ell, t)}{\partial L}\right) &= -\frac{\partial}{\partial L}\left(\frac{\left(\frac{\partial H(L,\ell,g,G(L,\ell,g,J_0))}{\partial L}\right)}{\left(\frac{\partial H(L,\ell,g,G(L,\ell,g,J_0))}{\partial G}\right)}\right) \\
&= -\frac{1}{\frac{\partial H}{\partial G}}\frac{\partial}{\partial L}\left(\frac{\partial H}{\partial L}(L, \ell, g, G(L, \ell, g, J_0))\right) \\
&\quad - \left(\frac{\partial H}{\partial L}\right)\left(\frac{1}{(\frac{\partial H}{\partial G})^2}\right) \cdot \frac{\partial}{\partial L}\left(\frac{\partial H}{\partial G}(L, \ell, g, G(L, \ell, g, J_0))\right) \\
&= -\frac{\left(\left(\frac{\partial H}{\partial G}\right)\left(\frac{\partial^2 H}{\partial L^2} + \frac{\partial^2 H}{\partial L \partial G}\frac{\partial G}{\partial L}\right) - \left(\frac{\partial H}{\partial L}\right)\left(\frac{\partial^2 H}{\partial L \partial G} + \frac{\partial^2 H}{\partial G^2}\frac{\partial G}{\partial L}\right)\right)}{(\frac{\partial H}{\partial G})^2}\,.
\end{aligned} \tag{40}$$

Note there is a $\frac{\partial G}{\partial L}$ to be dealt with. G is implicitly defined by

$$G = J_0 - \frac{1}{2L^2} + \Delta H(L, \ell, g, G(J_0, L, \ell, g)) \,. \tag{41}$$

Differentiate this expression to obtain

$$\frac{\partial G}{\partial L} = L^{-3} + \left(\frac{\partial \Delta H}{\partial L}\right) + \left(\frac{\partial \Delta H}{\partial G}\right)\left(\frac{\partial G}{\partial L}\right) \tag{42}$$

and solve to find

$$\frac{\partial G}{\partial L} = \frac{L^{-3} + \left(\frac{\partial \Delta H}{\partial L}\right)}{1 - \left(\frac{\partial \Delta H}{\partial G}\right)} \,. \tag{43}$$

One can now compute the partial derivatives of H using the equations of motion and plug everything into the above expression for $\frac{\partial}{\partial L}\left(\frac{\partial \tilde{H}_{J_0}(L,\ell,t)}{\partial L}\right)$. With the aid of a computer it is possible to estimate this term, which we call the *twist term*. Lets examine why this derivative is so important now.

4.2. **Proof of EAPT for the Return Map $\mathcal{F}$.** Since $\mathcal{F}$ arises as the Poincare return map of an autonomous Hamiltonian, it is area preserving, and also exact in that the area between a nonhomotopically trivial curve in $S(J_0)$ and its image under $\mathcal{F}$ is zero. The condition for twist for $\mathcal{F}$ is equivalent to $\frac{\partial \mathcal{F}_\ell}{\partial L_0} = \frac{\partial \ell(t^*, \ell_0, L_0)}{\partial L_0} < 0$ [Ban],[MF].

We now show that if $\frac{\partial}{\partial L}\left(\frac{\partial \tilde{H}_{J_0}(L,\ell,t)}{\partial L}\right) < 0$ then this corresponds to twist. Consider the equations of first variation.

$$\frac{d}{dt}\begin{pmatrix} \frac{\partial \ell}{\partial \ell_0} & \frac{\partial \ell}{\partial L_0} \\ \frac{\partial L}{\partial \ell_0} & \frac{\partial L}{\partial L_0} \end{pmatrix} = \begin{pmatrix} \frac{\partial^2 \tilde{H}_{J_0}}{\partial \ell \partial L} & \frac{\partial^2 \tilde{H}_{J_0}}{\partial L^2} \\ -\frac{\partial^2 \tilde{H}_{J_0}}{\partial \ell^2} & -\frac{\partial^2 \tilde{H}_{J_0}}{\partial \ell \partial L} \end{pmatrix} . \tag{44}$$

In particular, at time $t = 0$ it holds that

$$\frac{d}{dt}\left(\frac{\partial \ell}{\partial L_0}\right)\Big|_{t=0} = \frac{\partial^2 \tilde{H}_{J_0}}{\partial L^2}\Big|_{t=0} \,. \tag{45}$$

Hence the sign of $\frac{\partial^2 \tilde{H}_E}{\partial L^2}|_{t=0}$ determines whether $\frac{\partial \ell}{\partial L_0}$ is decreasing or increasing near $t = 0$. But $\frac{\partial \ell}{\partial L_0}|_{t=0} = 0$ so the sign of $\frac{\partial^2 \tilde{H}_{J_0}}{\partial L^2}$ will determine the sign of $\frac{\partial \ell}{\partial L_0}\big|_{t=0}$ in a neighborhood of $t = 0$, ie it will determine twist for the flow over a small increment of time. So if $\operatorname{sign}\left(\frac{\partial^2 \tilde{H}_{J_0}}{\partial L^2}\right)$ is constant for all $t \in [0, 2\pi]$, $\ell_0 \in \mathbb{T}$, and L_0 in some interval, then the map $\mathcal{F}$ is twisting in that region.

In the case $\mu = 0$, then $\frac{\partial F_\ell}{\partial L} = -\frac{\partial \ell}{\partial L_0} = -\frac{3}{L_0^4} \cdot 2\pi > 0$. Hence we require $\frac{\partial F_\ell}{\partial L_0} < 0$ for twist in RCP3BP. For $\mu > 0$, $\frac{\partial F_\ell}{\partial L} = -\frac{3}{L_0^4} \cdot 2\pi + O(\mu)$, and its possible for large L that the perturbation terms near the perihelion to overwhelm the $-\frac{3}{L_0^4}$ and change the sign of twist term. This is why twisting can fail.

With an explicit twisting condition, a computer can be programmed to look for sign changes in the twist term. For $J_0 = 1.8$ and $\mu = 0.001$, using nonrigorous numerics we see a sign change after $L = 16$, ie for eccentricities larger than 0.994 the map $\mathcal{F}$ may no longer be a twist map.

Lemma 4.1. *In Delauney variables, RCP3BP*$(0.001, 1.8)$ *is twisting for* $0.07 \leq e \leq 0.994$.

Remark. We have started using rigorous numerics to fully verify this result using interval arithmetic. The program is still running, however we are confident of the result based on high precision nonrigorous numerical evidence. In [GK2], we establish a coordinate system that is twisting for nearly parabolic motions and does not require this lemma.

5. Rigorous Action Comparison

We introduced several approximations in section 2 which, while reasonable sounding, are nonetheless not mathematically rigorous. We will rectify this now. It turns out that by using elliptic motions, we can lower $e(0.001, 1.8)$ down to $e = 0.66$ at the cost of increasing complexity of the estimates. This section relies on technical appendices and computer assisted methods for some of the estimates.

5.1. **The Intervalization of the RCP3BP.** The following formula nicely changes between time and radius.

$$\int_{t_0}^{t_1} dt = \int_{r_0}^{r_1} \frac{dr}{\dot{r}} \,. \tag{46}$$

This integral can be rearranged into the form

$$t_1 - t_0 = \int_{r_0}^{r_1} \frac{r dr}{\sqrt{2C(r^+ - r)(r - r^-)}} \tag{47}$$

$$r_+ = \frac{1 + \sqrt{1 - 2CP_\varphi^2}}{2C} \tag{48}$$

$$r_- = \frac{P_\varphi^2}{1 + \sqrt{1 - 2CP_\varphi^2}} \tag{49}$$

$$C = J_0 - P_\varphi + \Delta H \,. \tag{50}$$

In the case $\mu = 0$, the integral can be evaluated explicitly since then $\Delta H = 0$ and P_φ is constant. In the RCP3BP, we no longer have these luxuries as r^+ and r^- now depend on t, however we expect that in the outside region these quantities will not change much since the perturbative effects of Jupiter are too faint to make much of a difference. Our goal is to "intervalize" the problem, ie to use a

computer to generate rigorous bounds on the above terms and use interval arithmetic to manipulate the bounds.

The first step to carrying out this procedure is to get precise estimates on the perturbation terms. Using a computer, one can prove

Lemma 5.1. $|\Delta H| \leq \frac{2.7\mu}{r^3}$ *and* $|\frac{\partial \Delta H}{\partial r}| \leq \frac{12.5\mu}{r^4}$ *for* $r \geq 1.59$.

While this is adequate for exposition, it not quite accurate enough for our purposes. We define a function $(|\Delta H|)^+(r)$ so that for all $\varphi \in \mathbb{T}$ and $r \geq 1.59$ it holds that $(|\Delta H|)^+(r) \geq |\Delta H(r, \varphi)|$. The function $\left(\left|\frac{\partial \Delta H}{\partial r}\right|\right)^+(r)$ is defined similarly. In the appendix, we outline a method to define these functions precisely using a computer.

We also need very accurate estimates on how P_φ changes dynamically with time (or radius). In the appendix, we construct a function $\rho(r)$ such that $P_\varphi(t) \in P_\varphi(0) + [-\rho(r(t)), \rho(r(t))]$ for t the time between an apohelion and the following perihelion. Using ρ and some data from the rigorous integration (sect 5.7), one can prove the following lemma.

Lemma 5.2. *(Bounds on change in angular momentum)*
Assume $\mu = 10^-3$ *and* $J_0 = 1.8$. *Then*

(i) *When approaching the perihelion from the apohelion, angular momentum doesn't change by more than* $\rho(5) = 0.0215298\mu$ *over the entire outside region.*

(ii) *When approaching the perihelion from the apohelion, angular momentum doesn't change by more than* 4.44885μ.

(iii) *Angular momentum won't change by more than* 1.444μ *after an R-Solar passage.*

Furthemore, one can also prove

Lemma 5.3. $\rho(r) \leq \frac{20\mu}{r^3}$ *for* $r \geq 1.61$. *Furthermore* $\rho(r) \leq \frac{2.7\mu}{r^3}$ *for* $r \geq 5$.

This should not come as a great surprise since $P_\varphi - P_\varphi(0) = \int_0^t -\frac{\partial \Delta H}{\partial \varphi} dt$, so angular momentum changes solely due to the perturbation term which is of order $O(\frac{\mu}{r^3})$.

5.2. **New Outside Region Setup.** Assuming there is always parabolic behavior away from the sun is unnatural for low eccentricity orbits where the comet does not make large R-Solar passages. It more accurate to use elliptic orbits. From the formulas for $\lambda_\pm$ in section 2, we observe that it is in our favor to have time in the outside region as large as possible since this pushes $\lambda_\pm$ closer to one. By Kepler's Second Law, the comet will move the slowest, and hence take the most time near an apohelion. So when constructing the test curve γ_{test}, instead of $(5, R)$ and $(R, 5)$ segments, we use the pieces of trajectory connecting 5-Solar

passages, ie we start at $r = 5$, advance to an apohelion, and move back to $r = 5$ (fig. 9).

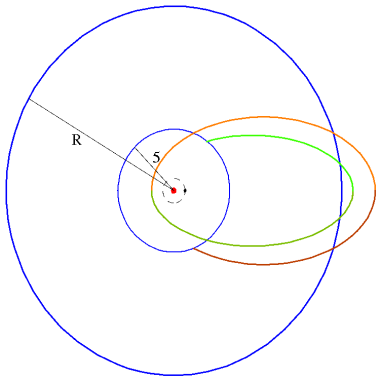

FIGURE 9. The New Outside Region Setup.

5.3. **Asymmetry in the Outside Region.** When approximating the RCP3BP with parabolic motions we made use of the fact that the 2BP before and after a 5-Solar passage were the same. This is not true in general. When the comet passes through the kick region, Jupiter changes the angular momentum of the comet. This changes the behavior of the comet in the outside region. In fact, this is the mechanism which allows capture and escape to occur. However this is difficult to model as the change in angular momentum after a 5-Solar passage means the apohelions before and after the 5-Solar passage are different. This means that γ^- and γ^+ spend different amounts of time in the outside region, and hence λ_- and λ_+ are not directly related.

Another technical complexity to consider is that our rigorous numerics work by taking intervals in initial conditions and integrating them (see appendix 8), in particular the integrator starts a comet at $r = 5$ and makes a 5-Solar passage. Let $P_\varphi(t_5)$ denote the angular momentum at the start of the 5–Solar passage. We consider $P_\varphi(t_5) \in \mathcal{I}$ and denote the enclosure for the angular momentum before the 5–Solar passage $\mathcal{I}_-$ and after $\mathcal{I}_+$. Note that we have $\mathcal{I} \subset \mathcal{I}_\pm$.

In order to reach the interval $\mathcal{I}$ at time t_5, initial conditions must be contained in $\mathcal{I} + [-2\rho(5), 2\rho(5)] = \mathcal{I}_-$ since this accounts for a change in angular momentum in the outside region. The bound of $2\rho(5)$ is because the comet passes between $r = 5$ and the apohelion twice.

Let $(\Delta P_\varphi)_{kick}(\mathcal{I})$ denote enclosure of possible changes in angular momentum after passing through the kick region when entering with angular momentum $P_\varphi \in \mathcal{I}$. This means that when leaving, $P_\varphi \in \mathcal{I} + (\Delta P_\varphi)_{kick}(\mathcal{I})$. Then when the

comet is leaving the sun and is in the outside region, $P_\varphi \in \mathcal{I} + (\Delta P_\varphi)_{kick}(\mathcal{I}) + [-2\rho(5), 2\rho(5)] = \mathcal{I}_+$.

5.4. **Some Bounds.** We are tasked with estimating all of equations (47) in detail. Suppose $\mathcal{I} = P_\varphi^* + [-w, w]$ and $|(\Delta P_\varphi)_{kick}(\mathcal{I})| \leq M$. We call $[-w, w]$ the *window* around P_φ^*. It is an artifact of the rigorous numerics. We use the $()^\pm$ to denote upper and lower bounds (see appendix 8). Lower case letters will denote values before the 5-Solar passage and upper case letters will denote values after the 5-Solar passage. Then let

$$c^\pm = J_0 - P_\varphi^* \pm 2\rho(5) \pm w \pm (|\Delta H|)^+(5) \tag{51}$$

$$C^\pm = J_0 - P_\varphi^* \pm 2\rho(5) \pm w \pm M \pm (|\Delta H|)^+(5)\,. \tag{52}$$

Clearly the above quantities bound $C = J_0 - P_\varphi + \Delta H$ before and after the 5-Solar passage. Consider the Sun-Comet two body problems with $P_\varphi = P_\varphi^* \pm \rho(5) \pm w$ or $P_\varphi = P_\varphi^* \pm \rho(5) \pm w \pm M$. We call the 2BPs with these angular momenta the *extreme 2BPs* with respect to P_φ^*. The RCP3BP with $P_\varphi(0) = P_\varphi^*$ has angular momenta between the values of the angular momenta for the extreme 2BPs with respect to P_φ^* Hence time spent in the outside region as well as action in the outside region for the RCP3BP is between the values found using the extreme 2BPs. For small w, we note that the range of angular momenta is not more than 3μ between the extreme 2BPs, so in the outside region away from parabolic motions ($e \leq 0.96$), there will not be any qualitative difference from using the extreme 2BP approximations. Hence in order to carry out the action comparison rigorously using the elliptic motions for RCP3BP, we carry it out for the extreme 2BPs and note that the actual value for RCP3BP will be contained inside bounds obtained. Now let

$$r_-^\pm = \frac{(P_\varphi^* \pm 2\rho(5) \pm w)^2}{1 + \sqrt{1 - 2(c^\pm)(P_\varphi^* \pm 2\rho(5) \pm w)^2}} \tag{53}$$

$$r_+^\pm = \frac{1 + \sqrt{1 - 2(c^\mp)(P_\varphi^* \mp 2\rho(5) \mp w)^2}}{2(c^\mp)} \tag{54}$$

$$R_-^\pm = \frac{(P_\varphi^* \pm 2\rho(5) \pm w \pm M)^2}{1 + \sqrt{1 - 2(C^\pm)(P_\varphi^* \pm 2\rho(5) \pm w)^2}} \tag{55}$$

$$R_+^\pm = \frac{1 + \sqrt{1 - 2(C^\mp)(P_\varphi^* \mp 2\rho(5) \mp w \mp M)^2}}{2(C^\mp)}\,. \tag{56}$$

In light of the integrals in appendix 11, we note that for the 2BP, time from the apohelion to $r = 5$ is given by

$$T_{out} = \frac{I_1(r^{perih}, r^{apoh}, 5, r^{apoh})}{\sqrt{2(E - P_\varphi)}}\,. \tag{57}$$

For RCP3BP, we let t_{out} be the time γ^- spends in the outside region, ie the time spent from initial conditions until the start of 5-Solar passage. Let T_{out} be the time γ^+ spends in the outside region, ie the time spent from the end of 5-Solar passage until the final conditions.

Lets use the estimates on P_φ, ΔH, r^{perih}, and r^{apoh} to estimate quantities in the action comparison. Define

$$b^{\pm}_{out}(k) = \frac{I_k(r^{\pm}_-, r^{\mp}_+, 5, r^{\mp}_+)}{\sqrt{2(c^{\mp})}} \tag{58}$$

$$B^{\pm}_{out}(k) = \frac{I_k(R^{\pm}_-, R^{\mp}_+, 5, R^{\mp}_+)}{\sqrt{2(C^{\mp})}} \tag{59}$$

where the I_k are integrals defined in the appendix. The signs of the radii are choosen so that they are all consistent with using a single extreme 2BP for each of the 4 possible bounds $b^{\pm}_{out}$, $B^{\pm}_{out}$. It follows that $t_{out} \in [2b^-_{out}(1), 2b^+_{out}(1)]$ and $T_{out} \in [2B^-_{out}(1), 2B^+_{out}(1)]$. Recall that the factor of 2 comes from the fact the distance from $r = 5$ to an apohelion is traversed twice in the new scheme for the outside region. The other values of k will used later.

5.5. λ **estimates.** If $(r(t), \varphi(t), \dot r(t), \dot\varphi(t))$ is a solution to the Euler-Lagrange equations, then the rescaled trajectory $\big(r(\frac{t}{\lambda}), \varphi(\frac{t}{\lambda}), \lambda\dot r(\frac{t}{\lambda}), \lambda\dot\varphi(\frac{t}{\lambda})\big) = (r_\lambda(t), \varphi_\lambda(t), \dot r_\lambda(t), \dot\varphi_\lambda(t))$ is also a solution to the Euler-Lagrange equations. The equations of motion give

$$\dot\varphi = -1 + \frac{P_\varphi}{r^2} \tag{60}$$

$$\dot\varphi_\lambda = \left(-1 + \frac{P_\varphi}{r^2}\right)\lambda\,. \tag{61}$$

Hence

$$\varphi(t) = \varphi(0) - t + \int_0^t \frac{P_\varphi(s)}{r(s)^2} ds \tag{62}$$

$$\varphi_\lambda(t) = \varphi(0) - \lambda t + \lambda\int_0^t \frac{P_\varphi(s)}{r(s)^2} ds\,. \tag{63}$$

We compute the differences in angle over time and solve for λ to get

$$\lambda(t) = 1 - \frac{\varphi_\lambda(t) - \varphi(t)}{t - \int_0^t \frac{P_\varphi(s)}{r^2(s)} ds}\,. \tag{64}$$

This formula can be interpreted as telling us how much of a rescaling λ is needed if we specify the difference $\big(\varphi_\lambda(t)-\varphi(t)\big)$ of angles from the rescaled and original trajectories at time t. Note that when using this formula, it is more convenient to calculate $\Delta\varphi(t_5)$, the difference in angles at the start of the 5-Solar passage, rather than $\Delta\varphi^{perih}$. This is because we want to compute time and action in the outside region only and the above formula allows us to consider behaviors only in the outside region. Using $\Delta\varphi(t_5)$ has the effect of redefining φ^{perih}_{max} and φ^{perih}_{min}. We now consider these angles to be the angle the comet makes with respect to Jupiter when at $r=5$ that respectively maximizes or minimizes A_{in} as in section 2.5. These angles depend on P_φ, as does the difference $\Delta\varphi(t_5)=\varphi^{perih}_{max}-\varphi^{perih}_{min}=\big(\varphi_\lambda(t)-\varphi(t)\big)$. It is acceptable to use this new difference in angles since solutions with these new minimal and maximal angles will flow into solutions with perihelion angles which minimize or maximize action.

Now lets estimate $\lambda_\pm$ using each of the extremal 2BPs listed above. First estimate,

(65)
$$\int_0^t \frac{P_\varphi(s)}{r^2(s)}ds=\int_{r(0)}^{r(t)}\frac{dr}{\dot r r^2}=\int_{r_0}^{r_1}\frac{P_\varphi dr}{\sqrt{2(J_0-P_\varphi+\Delta H)r(r^{apoh}-r)(r-r^{perih})}}$$

which looks like the integral I_{-1} from the appendix multiplied by P_φ. Let

$$j=[(P^*_\varphi-2\rho(5)-w)\cdot b^-_{out}(-1),(P^*_\varphi+2\rho(5)+w)\cdot b^+_{out}(-1)] \tag{66}$$

$$J=[(P^*_\varphi-2\rho(5)-w-M)\cdot B^-_{out}(-1),(P^*_\varphi+2\rho(5)+w+M)\cdot B^+_{out}(-1)]\,. \tag{67}$$

Then

$$\lambda^\pm_-(\mathcal{I}_-)\in 1-\frac{(\Delta\varphi(t_5))(\mathcal{I})}{2[b^-_{out}(1),b^+_{out}(1)]-2j} \tag{68}$$

$$\lambda^\pm_+(\mathcal{I}_+)\in 1+\frac{(\Delta\varphi(t_5))(\mathcal{I})}{2[B^-_{out}(1),B^+_{out}(1)]-2J}\,. \tag{69}$$

The signs in $\lambda^\pm_\pm$ come about by examining the action comparion in the kick region and noting the maximal action comes after the minimal one (ie it is less than π to the right of the minimal action, and more than π to the left on the circle.) Then starting at the maximal action, we need to slow down the comet, ie we need $\lambda_-<1$. Thinking of this another way, since $\dot\varphi<0$, slowing down means spending more time in the outside region, which means φ decreases.

5.6. **Action Decomposition.** Using $H=-E=J_0$, it follows that for elliptic motions $\frac{v^2}{2}=\frac{P_r^2}{2}+\frac{P_\varphi^2}{2r^2}=\frac{1}{r}+\Delta H-E+P_\varphi$ where $v=\dot\gamma$. The rescaled action for

the elliptic case is

$$A(\lambda, t_0, t_1 = \int_{t_0\lambda}^{t_1\lambda} \left(\frac{\lambda^2 v^2}{2} + \frac{1}{r} - \Delta H\right)\left(\frac{t}{\lambda}\right) dt \tag{70}$$

$$= \lambda \int_{t_0}^{t_1} \left(\lambda^2\left(\frac{1}{r} + \Delta H - E + P_\varphi\right) + \frac{1}{r} - \Delta H\right)(u) du \tag{71}$$

$$= \int_{t_0}^{t_1} \frac{\lambda^3 + \lambda}{r} dt + \int_{t_0}^{t_1} \lambda^3(-E + P_\varphi) dt + \int_{t_0}^{t_1} (\lambda^3 + \lambda)(-\Delta H) dt\,. \tag{72}$$

We define

$$A_P(\lambda, t_0, t_1) = \int_{t_0}^{t_1} \frac{\lambda^3 + \lambda}{r} dt \tag{73}$$

$$A_K(\lambda, t_0, t_1) = \int_{t_0}^{t_1} \lambda^3(-E + P_\varphi) dt \tag{74}$$

$$A_{\Delta H}(\lambda, t_0, t_1) = \int_{t_0}^{t_1} (\lambda^3 + \lambda)(-\Delta H) dt \tag{75}$$

so that $A = A_P + A_K + A_{\Delta H}$. To do the action comparison, we need to estimate

$$\begin{aligned} A(1, t_{out}) - A(\lambda_+, t_{out}) + A(1, t_{out}) - A(\lambda_-, t_{out}) \\ =& A_P(1, t_{out}) - A_P(\lambda_+, t_{out}) + A_P(1, t_{out}) - A_P(\lambda_-, t_{out}) \\ &+ A_K(1, t_{out}) - A_K(\lambda_+, t_{out}) + A_K(1, t_{out}) - A_K(\lambda_-, t_{out}) \end{aligned} \tag{76}$$

$$+ A_{\Delta H}(1, t_{out}) - A_{\Delta H}(\lambda_+, t_{out}) + A_{\Delta H}(1, t_{out}) - A_{\Delta H}(\lambda_-, t_{out})\,. \tag{77}$$

To estimate each of these terms, our strategy is to get lower and upper bounds by using the extreme 2BP's.

5.6.1. *$A_{\Delta H}$ estimates.* The least care needs to be taken in estimating this term.

$$A_{\Delta H}(1, t_{out}) - A_{\Delta H}(\lambda_+, t_{out}) + A_{\Delta H}(1, t_{out}) - A_{\Delta H}(\lambda_-, t_{out}) \tag{78}$$

$$= \int_{t_{out}} (2 - \lambda_+^3 - \lambda_+)(-\Delta H) dt + \int_{t_{out}} (2 - \lambda_-^3 - \lambda_-)(-\Delta H) dt \tag{79}$$

$$\in 2[B_{out}^-(1), B_{out}^+(1)](2 - [\lambda_+^-, \lambda_+^+]^3 - [\lambda_+^-, \lambda_+^+])[(|\Delta H|)^+(5)] \tag{80}$$

$$+ 2[b_{out}^-(1), b_{out}^+(1)](2 - [\lambda_-^-, \lambda_-^+]^3 - [\lambda_-^-, \lambda_-^+])[(|\Delta H|)^+(5)]\,.$$

This term is small, usually of the order $10\mu^2$, and no additional refinements need to be made to this estimate.

5.6.2. *A_K estimates.* Lets estimate

$$\begin{aligned} &A_K(1,t_{out})-A_K(\lambda_+,t_{out})+A_K(1,t_{out})-A_K(\lambda_-,t_{out}) \\ &\qquad = \int_{t_{out}} \left(1-\lambda_-^3\right)(-E+P_\varphi)dt + \int_{t_{out}} \left(1-\lambda_+^3\right)(-E+P_\varphi)dt \end{aligned} \tag{81}$$

using the extreme 2BPs. To keep notation simple, let $\min(\mathcal{I}_-)=m_-$, $\max(\mathcal{I}_-)=m_+$, $\min(\mathcal{I}_-)=M_-$, and $\max(\mathcal{I}_+)=M_+$.

$$\int_{t_{out}} \left(1-\lambda_-^3\right)(-E+P_\varphi)dt + \int_{T_{out}} \left(1-\lambda_+^3\right)(-E+P_\varphi)dt \tag{82}$$

$$\subset \left[2\cdot\left(b_{out}^-(1)\right)\cdot\left(1-(\lambda_-^-)^3\right)\cdot\left(-E+m_-\right),\ 2\cdot\left(b_{out}^+(1)\right)\cdot\left(1-(\lambda_-^+)^3\right)\cdot\left(-E+m_+\right)\right]$$

$$+\left[2\cdot\left(B_{out}^-(1)\right)\cdot\left(1-(\lambda_+^+)^3\right)\cdot\left(-E+M_-\right),\ 2\cdot\left(B_{out}^+(1)\right)\cdot\left(1-(\lambda_+^-)^3\right)\cdot\left(-E+M_+\right)\right]. \tag{83}$$

Note the ordering of the bounds. For example $b_{out}^-(1)$ is paired with λ_-^- and m_- since smaller angular momentum means a smaller apohelion, meaning less time is spent in the outer region, ie a smaller t_{out}, and less time in the outer region means a worse λ value, ie farther from one, ie a smaller $\lambda_-<1$. The logic for the other pairings is similar.

These bounds are readily computable on a computer.

5.6.3. *A_P estimates.* Now estimate

$$\begin{aligned} &A_P(1,t_{out})-A_P(\lambda_+,t_{out})+A_P(1,t_{out})-A_P(\lambda_-,t_{out}) \\ &\qquad = \int_{t_{out}} \frac{2-(\lambda_-^3+\lambda_-)}{r}dt + \int_{t_{out}} \frac{2-(\lambda_+^3+\lambda_+)}{r}dt \end{aligned} \tag{84}$$

using the extreme 2BPs. Note that these integrals look like I_0 from the appendix. To keep notation simple, let $\min(\mathcal{I}_-)=m_-$, $\max(\mathcal{I}_-)=m_+$, $\min(\mathcal{I}_-)=M_-$, and $\max(\mathcal{I}_+)=M_+$.

$$\int_{t_{out}} \frac{2-(\lambda_-^3+\lambda_-)}{r}dt + \int_{t_{out}} \frac{2-(\lambda_+^3+\lambda_+)}{r}dt \tag{85}$$

$$\subset \left[2\cdot\left(b_{out}^-(0)\right)\cdot\left(2-(\lambda_-^-)^3-\lambda_-^-\right), 2\cdot\left(b_{out}^+(0)\right)\cdot\left(2-(\lambda_-^+)^3-\lambda_-^+\right)\right]$$

$$+\left[2\cdot\left(B_{out}^+(0)\right)\cdot\left(2-(\lambda_+^-)^3-\lambda_+^-\right), 2\cdot\left(B_{out}^-(0)\right)\cdot\left(2-(\lambda_+^+)^3-\lambda_+^+\right)\right]. \tag{86}$$

These bounds are readily computable on a computer.

5.7. **The Kick Region Action Comparison.** In this subsection we consider $\mu = 10^{-3}$ and $J_0 = 1.8$ and develope precise estimates on how action varies in the kick region. We program the CAPD package to rigorously integrate trajectories over 5-Solar passages, and record $\Delta A_{in}^{min}(\mathcal{I})$, $\Delta\varphi(t_5)(\mathcal{I})$, the change in angular momentum over the kick region $(\Delta P_\varphi)_{kick}(\mathcal{I})$, and the time to cross the kick region. Stated as a theorem

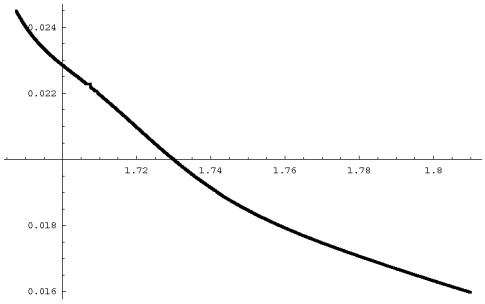

FIGURE 10. Lower bounds on $\Delta A_{in}^{min}(P_\varphi)$ vs. P_φ.

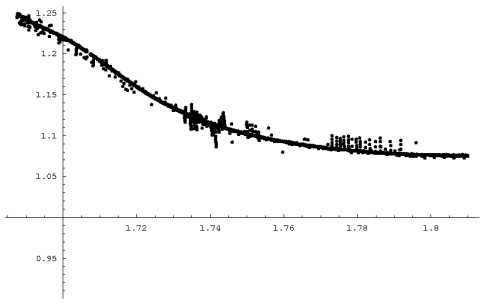

FIGURE 11. Upper bounds on $\Delta\varphi(t_5)(P_\varphi)$ vs. P_φ.

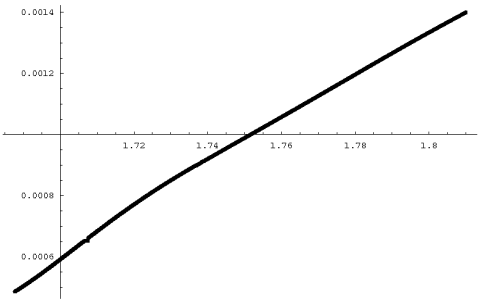

FIGURE 12. Upper bounds on $(\Delta P_\varphi)_{kick}$ vs. P_φ.

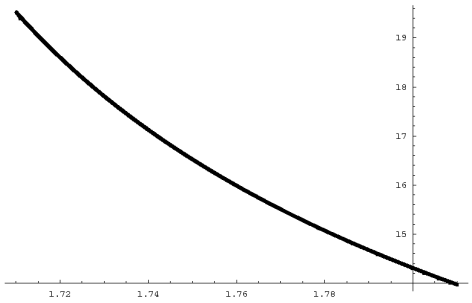

FIGURE 13. Upper bounds on the maximum time to cross the kick region.

Theorem 5.4. *For RCP3BP*$(0.001, 1.8)$ *and* $P_\varphi \geq 1.6875$*,*

$$\Delta A_{in}^{min} \geq 15.9748\mu \tag{87}$$

$$\Delta\varphi(t_5) \leq 1.2495 \tag{88}$$

$$|(\Delta P_\varphi)_{kick}| \leq 1.40093\mu\,. \tag{89}$$

Furthermore, for $P_\varphi \geq 1.71$*, the maximum time to cross the kick region is less than* 19.5256*.*

Proof. We program the CAPD package to rigorously integrate trajectories over a 5-Solar passage. Action can also be solved for simultaneously by noting that since action is the integral of the Lagrangian, i.e. $A(t) = \int_0^t L(s)ds$, hence $\dot{A} = L(t)$, and $L(t)$ depends on the polar variables at time t, which are known after one step of the integrator. Use initial conditions $r = 5$, $P_\varphi \in [1.6875, 1.81]$, $\varphi \in \mathbb{T}$. Subdivide $[1.6875, 1.81]$ into 4901 boxes of size 0.000025, and subdivide $[-\pi, \pi]$ into 12567 boxes of size 0.000025. Use the implicit definition of $P_r = \sqrt{2\big(1.8 - \frac{P_\varphi^2}{2r^2} + \frac{2}{r} - \Delta H(r,\varphi)\big)}$ on the energy surface $\mathcal{S}(1.8)$. Use $A(0) = 0$. Integrate trajectories until they cross $\{r = 5\}$ again. Record the action before and after the box of trajectories crosses $\{r = 5\}$. Then make an interval out of the lower and upper bounds on action while crossing. Since the box is small, with the use of adaptive step size, the width of the action interval will be small, and it accurately measures action for the box being integrated. We do this for each trajectory with a fixed box of P_φ's, i.e. for $P_\varphi(t_5) \in P_\varphi^* + [-w, w]$. The action difference in this class is bounded using the largest lower bound of all the action intervals, and smallest upper bound. Actual differences could be larger. Also recorded is the angle of the initial conditions which produces each extremal box, the maximum change in angular momentum for each window of initial condition, and the exit times. This all gives the data above. Note that this method actually produces an extensive list of boxes and bounds. These are plotted in the graphs above.

Remark. This setup is expensive and took 15 computers 2 weeks to complete the comparison.

Using the above estimates for the outside region, as well as the rigorous integration data for the kick region, a program was written to compare action. The result is the estimate in the main theorem that $e^*(0.001, 1.8) \leq 0.66$. The software is general enough to handle other values of μ and J_0.

6. The applicability of Aubry-Mather Theory

We have shown that the map $\mathcal{F}$ is an exact area preserving twist map in Delauney coordinates. However the action comparison was performed in polar coordinates. We need

Theorem 6.1. *(Bernard's Theorem) If ϕ is a canonical change of coordinates on a smooth compact manifold M, then for every ω, the Aubry-Mather set Σ_ω contained in the domain of ϕ is preserved under the change of coordinates* [Ber].

Unfortunately, this theorem requires that Aubry-Mather (AM) sets are contained in compact domains. We need to know that in particular they won't leave the twist region, $e \leq 0.994$. The estimates on change in angular momentum tell us that making one full orbit (perihelion to perihelion) will not change angular momentum by more than 8.95μ (see appendix). Translating this into a statement about eccentricity, it says that starting with initial eccentricity $e \leq 0.96$, the comet remains in the twist region after one revolution around the sun. Hence starting in $e \leq 0.96$ will ensure our AM sets remain bounded safely inside the twist region. The AM sets are bounded below by invariant curves, say near $e = 0.3$ from the [CC] result. Hence all our AM sets are contained in a compact region. [GK3] provides more of a justification for this bound as well as develops more efficient methods for bounding the location of Σ_ω.

Let $\beta(L)$ be a C^∞ bump function which is 1 for $L \in [1.7, 16]$ (i.e. 1 for eccentricities between 0.3 and 0.994), and 0 outside of a neighborhood of $[1.7, 16]$. Now consider the dynamics of the Hamiltonian $H_{Del}^{3BP} \cdot \beta(L)$. It will behave like that of H_{Del}^{3BP} on the compact region $\{1.7 \leq L \leq 16\}$, and is trivial outside a neighborhood of this interval. Hence Bernard's Theorem applies using this compact subset of the energy surface. Thus Aubry-Mather sets will remain the same in both coordinate systems, so invariant 2-tori will be action minimizing by standard results for exact area preserving twist maps [Ban], [MF], [S].

If C_- and C_+ are two rotationally invariant curves such that there are no invariant curves in between C_- and C_+, we say that region C bounded by C_- and C_+ is a *Birkhoff Region of Instability* (BRI). Our main result says that we have a BRI inside of $e \in [0.66, 0.96]$. Furthermore,

Theorem 6.2. *(Mather Connecting Theorem) For any two rotation numbers $\omega, \omega' \in [\omega_-, \omega_+]$ inside of the rotation interval of a Birkhoff Region of Instability C, there is a point $p \in C$ such that the α limit set of p is contained in Σ_ω and the ω limit set of p is contained in $\Sigma_{\omega'}$.* ([K1], [Ma]).

Furthermore, every possible rotation number has an Aubry-Mather set associated to it [Ma]. Each eccentricity $e = e_0$ on the cylinder $\mathcal{S}(J_0) \cap \mathcal{H}(J_0) \cap \{g = g^*\}$ has a range of rotation numbers associated it. These are determined by the speed at which ℓ goes around the base $\mathbb{T}$, i.e. the speed at which the comet moves around the sun. Higher eccentricities will have smaller rotation numbers. Hence the Mather Connecting Theorem provides us with a connecting orbit which starts with initial eccentricity $e = 0.66$ and approaches eccentricity $e = 0.96$.

7. Conclusion and Extension

We have constructed a large Birkhoff region of instability. What prevents us from extending the result to eccentricities beyond e_{max} is the fact that our coordinate system becomes undefined for nearly parabolic motions. This is not an ideological issue as we expect instabilities near the separatrices which arise from parabolic motions. Delauney variables can be modified near the separatrices to deal with singularities which arise for nearly parabolic motions, and this is done in [GK2]. When done our claim becomes

Theorem 7.1. *Consider the restricted circular planar three body problem with Sun-Jupiter mass ratio μ. Fix a Jacobi Constant J that produces three disjoint Hill regions and consider dynamics in the outer Hill region. There exist trajectories of a comet with initial eccentricity $e^* = e(\mu, J)$ that increases in eccentricity beyond 1, i.e. the comet escapes the solar system to infinity. For example, if $\mu = 10^{-3}$ and $J = 1.8$, then $e^* \leq 0.66$.*

8. Appendix - Rigorous Numerics

We need a computer to provide mathematically verified bounds on flows of ODE's to complete some of the estimates encountered. Consider the initial value problem (IVP)

$$\begin{cases} \dot{x} & = f(x) \\ x(0) & = x_0 \end{cases} \tag{90}$$

Assume that solutions exist, are unique, and are defined for all time, and that f is sufficiently smooth (either C^∞ or real analytic). We specify a fixed step size h for the Euler Method. If $x(t)$ is a solution to the IVP, then from Taylor's Theorem

$$x(t+h) = x(t) + x'(t) + O(h^2) \approx x(t) + hf(x(t)) \tag{91}$$

Euler's Method forgets the remainder and makes the a linear approximation at each time step to give

$$\begin{cases} t_i &= t_{i-1} + h \\ x_i &= x_{i-1} + hf(x_{i-1}) \,. \end{cases} \tag{92}$$

Each step of the Euler Method makes an error of $O(h^2)$, known as the *local truncation error*, which for h small isn't too bad. However the small errors made by disregarding the $O(h^2)$ causes the method to track a slightly different solution each time step. After many steps these small errors can accumulate and destroy the method's usefulness by jumping to a solution which has different behavior from the one desired. This is known as *global truncation error*. Even higher order methods like Runge-Kutta 7-8 are still susceptible to this. We utilize methods which avoid these difficulties.

8.1. **Interval Arithmetic.** When working on a computer, there is another source of error which must be accounted for - floating point error - which arises because a computer is incapable of representing a general real number.

Machine representable numbers are a subset of real numbers which a computer can perform computations with. We define *machine-*ϵ as the smallest positive number such that $1 \neq (1+\epsilon)$ on our machine. It gives a kind of spacing between machine representable numbers. This is dependent on the computer's architecture and software, however most computers adopt IEEE standards which specify such representable numbers, and use machine $\epsilon \approx 10^{-16}$. Assume that we have adopted such a standard. [IEEE]

One method to get around these difficulties is by using so called interval arithmetic. If $x \in \mathbb{R}$ we say $[a,b]$ is an *interval representation* for x with machine representable numbers a and b if $x \in [a,b]$. We denote intervals in calligraphic capital letters ($\mathcal{I}$). If $\mathcal{I} = [a,b]$, then define $max(\mathcal{I}) = b$ and $min(\mathcal{I}) = a$.

If $f\colon \mathbb{R}^n \times \mathbb{R}^m \to \mathbb{R}$ is a smooth function and $\mathcal{I} \times \mathcal{J}$ is a product of intervals, we say that the interval $\mathcal{K}$ *encloses* f on the domain $\mathcal{I} \times \mathcal{J}$ if $f(\mathcal{I}, \mathcal{J}) \subset \mathcal{K}$. Computing good enclosures is a principle difficulty in interval arithmetic. [KM] and [MZ] contain methods to make enclosures both rigorous and efficient.

When we say "bound $f\colon \mathbb{R}^d \to \mathbb{R}$ over domain D using interval arithmetic" we really mean to use the following algorithm.

1) Cover D with n intervals (or products of intervals) $\mathcal{I}_i^d$ so that $D \subset \cup_i^n \mathcal{I}_i^d$.

2) Find enclosures $\mathcal{K}_i$ such that $f(\mathcal{I}_i^d) \subset \mathcal{K}_i$.

3) Compute $m = \min(\mathcal{K}_i)$ and $M = \max(\mathcal{K}_i)$

This algorithm gives numbers so that $m \leq f(D) \leq M$. Bounds depend on D, d, n, and the regularity of f. Generally speaking, decreasing $diam(\mathcal{I}_i^d)$ improves the bounds.

Several of our computations are done on a Computer Algebra System (CAS). Generally speaking, a *computer algebra system* is a system which rigorously manipulates algebraic and numerical expressions. A CAS can be programmed to use *exact arithmetic*, which is arithmetic using symbolic expressions to produce exact output without rounding. For example $\frac{1}{2} + \frac{1}{3} = \frac{5}{6}$ on a CAS. It is possible to perform exact interval arithmetic where intervals contain symbolic expressions and the bounds are manipulated using exact arithmetic. Our CAS needs the following capabilities.

1) Manipulates algebraic expressions using exact arithmetic

2) Take symbolic derviatives (where possible)

3) Take symbolic integrals (where possible)

4) Perform interval arithmetic accounting for rounding error

Remark. Mathematica is one such CAS which satisfies these constraints. There are others.

As we will be computing many lower and upper bounds, lets adopt the notation $(\cdot)^{\pm}$ to denote functions or numbers which are upper and lower bounds on the function $(\cdot)$. For example $f(x,y) \leq (f(x))^{+}$ means that $(f(x))^{+}$ is a function of x such that the bound holds for all y in the domain of f.

Returning to the problem of rigorous numerics for ODE's, we reformulate the problem in terms of interval arithmetic. Now consider the *Interval Value Problem (IvVP)* .

$$\begin{cases} \dot{x} & = f(x) \\ x(0) & \in I \end{cases} \tag{93}$$

where now I is some interval of initial conditions, x is now made up of interval objects instead of reals, and all operations are performed via interval arithmetic. From a dynamical systems perspective, we seek to transport a cube of initial conditions under the flow of the ODE. The advantage of an IvVP solver is that by covering the space of initial conditions with intervals, the solver tells us rigorously how the entire space moves under flow.

8.2. **The Lohner Algorithm.** One might wonder how to construct a rigorous IvVP solver or even if they exist. Both questions are answered in [Z] and [WZ]. The main idea is as follows.

Notice the difficulty with nonrigorous methods is that they follow slightly different solutions at each step which gradually move apart. Gronwall's inequality tells us that differing solutions move apart at most exponentially based on the magnitude of a Lipschitz constant, which is roughly $||Df(x)||$. The $O(h^2)$ truncation error in Euler's Method is from remainder term in the Taylor's theorem which can be written in the form $x''(\xi)\frac{h^2}{2} = Df(\xi)f(\xi)\frac{h^2}{2}$ for some ξ. A naive way to produce a rigorous integrator is to bound the truncation error at each step. Poor bounds will require the integrator to use larger interval bounds at each step, and these bounds can potentially grow exponentially, rendering the output useless. This is commonly known as the *wrapping effect*.

In order to get good estimates on the errors made, accurate of estimates of $||Df(x)||$ are needed. One way to do this is to solve the equations of first variation rigorously. Any bound on the variational equations will suffice to rigorously take a step in the Euler Method. In [Z], [WZ] and [MZ], efficient methods are outlined. They introduce efficient representations of interval sets that allow for better bounds. It is also noted that in solving the equations of variation, the same main idea can be applied to $D^2f(x)$ and higher derivatives so that one can get efficient bounds for higher order equations of variation.

The theory developed in [Z] and [WZ] has been implemented in a package called CAPD. It is our primary tool for rigorous integration of the equations of motion.

9. Appendix-Estimates on Perturbation Terms

We outline how a computer can generate $(|\Delta H|)^+(r)$ and $\left(\left|\frac{\partial \Delta H}{\partial r}\right|\right)^+(r)$.

9.1. **Outside Region Estimates.**

Step 1a – First Taylor expand in $\frac{1}{r}$ the perturbation term ΔH to 12 terms, and $\frac{\partial \Delta H}{\partial r}$ to 13 terms. The coefficients are trigonometric polynomials in φ.

Step 1b – Using basic calculus (or a CAS), find the maximum of the absolute value of the coefficients. Exact interval arithmetic can also be used to do this.

Step 1c – Compute the remainder terms. They are functions of $\frac{1}{r}$ and φ. Both are defined on compact domains, $0 \leq \frac{1}{r} \leq \frac{1}{5}$ and $-\pi \leq \varphi \leq \pi$. Note that ΔH and $\frac{\partial \Delta H}{\partial r}$ have critical points at $\varphi = 0, \pi$ and $\cos(\varphi) = \frac{1-2\mu}{2r}$ hence so do their derivatives in $\frac{1}{r}$. Subdivide the domain $0 \leq \frac{1}{r} \leq \frac{1}{5}$ into intervals of size 10^{-3} and use exact interval arithmetic to obtain rigorous upper bounds on the remainder term.

Step 1d – Assemble new terms which are the Taylor Polynomials from **1a** with the coefficients from **1b** and the remainder terms from **1c**. We use these to define the symbols $(|\Delta H|)^+$ and $\left(\left|\frac{\partial \Delta H}{\partial r}\right|\right)^+$ for $r \geq 5$.

Remark. All of these estimates are independent of the Jacobi constant.

Some of the leading terms in the expansion for $r \geq 5$.

$$(|\Delta H|)^+ = \frac{\mu(1-\mu)}{r^3} + \frac{\mu(1-\mu)(1-2\mu)}{r^4} + \ldots \text{ for } r \geq 5 \tag{94}$$

$$\left(\left|\frac{\partial \Delta H}{\partial r}\right|\right)^+ = \frac{3\mu(1-\mu)}{r^4} + \frac{4\mu(1-\mu)(1-2\mu)}{r^5} + \ldots \text{ for } r \geq 5 \tag{95}$$

Remark. While the leading terms are able to be expressed in terms of μ for any value of μ explicitly, later terms which the computer find will depend on the specific μ used. However the software written is general enough to handle any input μ.

9.2. **Kick Region Estimates.** We modify the above technique to estimate the perturbation terms in the kick region, where the bounds on the remainder term become poor for $r < 5$.

Step 1e – Keep the terms up to order 5 for $(|\Delta H|)^+$ and order 6 for $\left(\left|\frac{\partial \Delta H}{\partial r}\right|\right)^+$ from the outside region, and add new remainder terms of the form $\frac{1}{300r^6}$ and $\frac{1}{50r^7}$ respectively.

We use these new functions to define the symbols $(|\Delta H|)^+$ and $\left(\left|\frac{\partial \Delta H}{\partial r}\right|\right)^+$ in the kick region. Interval arithmetic is used to verify the approximations generated are bounds on the actual perturbation terms.

Remark. The estimates for the inner region where found by hand for the specific value of $\mu = 10^{-3}$. However it is possible to program the CAS to find estimates in the kick region for any value of μ.

9.3. **Assumptions and Some Initial Bounds.** Consider the case $\mu = 10^{-3}$ and $J_0 = 1.8$. It is useful to have some initial bounds on angular momentum and minimal radius. Note that the class of solutions we care about has $P_\varphi \leq 1.81$, i.e. $e \leq 1.0324$. For now we assume that $P_\varphi \leq 1.81$, and justify this later.

Noting that $P_\varphi = (r^{perih})^2 - \sqrt{2(r^{perih}) - 2\Delta H - 2E(r^{perih})^2 + (r^{perih})^4}$, then one gets an upper bound on P_φ by using $(|\Delta H|)^+$ in place of ΔH in the definition of P_φ. Further examination indicates that increasing P_φ decreases r^{perih}. Hence its possible to get a lower bound on r^{perih}, which can be used to bound the magnitude of the perturbation term.

$$r^{perih} \geq 1.61048 = r^{perih}_{min} \tag{96}$$

$$|\Delta H| \leq 0.629522\mu\,. \tag{97}$$

We justify our assumptions in the next section.

10. Appendix – Estimates on change in P_φ

We prove lemma 5.2. It will become necessary to have good estimates on how P_φ changes. Recall that

$$\dot{P}_\varphi = -\frac{\partial \Delta H}{\partial \varphi}\,. \tag{98}$$

Hence

$$\Delta P_\varphi(t_0,t_1) = P_\varphi(t_1) - P_\varphi(t_0) = \int_{t_0}^{t_1} -\frac{\partial \Delta H}{\partial \varphi} dt\,. \tag{99}$$

Now

$$\frac{d}{dt}\Big(\Delta H(r(t),\varphi(t))\Big) = \left(\frac{\partial \Delta H}{\partial r}(t)\right)\dot{r}(t) + \left(\frac{\partial \Delta H}{\partial \varphi}(t)\right)\dot{\varphi}(t) \tag{100}$$

and hence

$$\frac{\partial \Delta H}{\partial \varphi}(t) = \frac{1}{\dot{\varphi}(t)}\Big(\frac{\partial \Delta H}{\partial r}(t)\dot{r}(t) - \frac{d}{dt}(\Delta H(t))\Big)\,. \tag{101}$$

Plugging in and using a change of variables gives

$$\Delta P_\varphi(t_0,t_1) = \int_0^t -\frac{1}{\dot{\varphi}(t)}\Big(\frac{\partial \Delta H}{\partial r}(t)\dot{r}(t) - \frac{d}{dt}\Delta H(t)\Big)dt$$

$$= \int_0^t \frac{1}{\dot{\varphi}(t)}\Big(\frac{d}{dt}\Delta H(t)\Big)dt - \int_{r(t_0)}^{r(t_1)} \frac{1}{\dot{\varphi}(t(r))}\Big(\frac{\partial \Delta H}{\partial r}\Big)\Big(r,\varphi(t(r))\Big)dr\,. \tag{102}$$

Let $r_0 = r(t_0)$ and $r_1 = r(t_1)$. Suppose the comet is *approaching the perihelion from the apohelion*. Then $r_1 \leq r_0$. As t increases, r decreases, and our estimate should account for more uncertainty in the value of P_φ given the perturbation term grows larger in magnitude closer to the sun.

$$|\Delta P_\varphi(t_0,t_1)| \leq \frac{1}{\min_{r\in[r_0,r_1]}|\dot{\varphi}(r)|}\left(\Big|\int_{t_0}^{t_1}\frac{d}{dt}\Delta H(t)dt\Big| + \int_{r_1}^{r_0}\Big|\frac{\partial \Delta H}{\partial r}\Big|dr\right) \tag{103}$$

Note that

$$\min_{r\in[r_0,r_1]}|\dot{\varphi}(r)| \geq \min_{r\in[r_0,r_1]}\Big(1-\frac{P_\varphi}{r^2}\Big) \geq 1 - \frac{\max P_\varphi}{r_1^2}\,. \tag{104}$$

Hence

$$|\Delta P_\varphi(t_0,t_1)| \leq \frac{1}{1-\frac{\max P_\varphi}{r_1^2}}\Big(|\Delta H(t_1)-\Delta H(t_0)| + \int_{r_1}^{r_0}\Big|\frac{\partial \Delta H}{\partial r}\Big|dr\Big) \tag{105}$$

$$\leq \frac{1}{1-\frac{\max P_\varphi}{r_1^2}}\Big((|\Delta H|)^+(r_0) + (|\Delta H|)^+(r_1) + \int_{r_1}^{r_0}\left(\Big|\frac{\partial \Delta H}{\partial r}\Big|\right)^+ dr\Big)\,. \tag{106}$$

Claim. $\left((|\Delta H|)^+(r_0) + (|\Delta H|)^+(r_1) + \int_{r_1}^{r_0} \left(\left|\frac{\partial \Delta H}{\partial r}\right|\right)^+ dr\right)$ is nondecreasing as a function of r_0 for $r_0 \geq 1.59$.

Since $(|\Delta H|)^+$ is decreasing as a function of r and $\lim_{r_0\to\infty}(|\Delta H|)^+(r_0) = 0$, from this claim it follows that

(107)

$$|\Delta P_\varphi(t_0, t_1)| \leq \rho(r(t_1)) := \frac{1}{1 - \frac{\max P_\varphi}{r_1^2}}\left((|\Delta H|)^+(r_1) + \int_{r_1}^{\infty} \left(\left|\frac{\partial \Delta H}{\partial r}\right|\right)^+ dr\right)$$

provided that the radius is decreasing from t_0 to t_1 and the comet is in the outside region. Using $(\max P_\varphi) \leq 1.81$ to evaluate $\rho(5)$ gives an upper bound on the change of P_φ over the whole outside region. Note that this argument can be made symmetric by considering change from the final conditions and reserving time. Hence, (i) when approaching the perihelion from the apohelion, angular momentum doesn't change by more than $\rho(5) \approx 0.0215298\mu$ over the entire outside region, (ii) when approaching the perihelion from the apohelion, angular momentum doesn't change by more than $\rho(r_{min}^{perih}) \approx 4.44885\mu$, and (iii) angular momentum won't change by more than $2\rho(5) + 2\rho(r_{min}^{perih}) \approx 8.94077\mu$ during an R-Solar passage.

If we only care about change in angular momentum after an R-Solar passage, then (iii) is not an optimal bound. We use CAPD to perform rigorous integration over all 5-Solar passages with $P_\varphi \in [1.68753, 1.81]$ and note that $|\Delta P_\varphi| \leq 1.4\mu$ (Theorem 5.4). Thus a more tight estimate on total change in angular momemtum after an R–Solar passage is $1.4\mu + 2 \cdot 0.0215298\mu < 1.444\mu$.

This justifies the initial assumption, since if the comets starts with $P_\varphi(0) = 1.8$ (i.e. $e = 1$) and approached the sun to make an R-Solar passage, then the most angular momentum could ever be is $P_\varphi = 1.80894077 < 1.81$. Note that $e \leq 0.96$ corresponds to $P_\varphi \leq 1.788$.

Remark. We have implicitly used $J_0 = 1.8$ and $\mu = 10^{-3}$ to generate the estimate on change in angular momentum since these constants are used in estimates on ρ, $(|\Delta H|)^+$, and $\left(\left|\frac{\partial \Delta H}{\partial r}\right|\right)^+$. The software to estimate these quantities will accept any μ and J_0 and the estimates on the integral above is general in nature, so similar estimates on change in angular momentum for any μ and J_0 where there are three disjoint Hill regions with dynamics in the outer Hill region can be generated by the computer.

11. Appendix - Estimations of Common Integrals

We need to know some properties of the following commonly occurring integrals. At various times one encounters integrals of the form

$$\int_{t_0}^{t_1} r^k(t)dt = \int_{r_0}^{r_1} \frac{r^k dr}{\dot{r}}\,. \tag{108}$$

Rewriting this

$$F(J_0, r_0, r_1, P_\varphi, k) = \int_{r_0}^{r_1} \frac{r^{k+1}dr}{\sqrt{2(J_0 - P_\varphi + \Delta H)(r_+ - r)(r - r_-)}}\,. \tag{109}$$

Suppose that we can bound $2(E - P_\varphi + \Delta H)$ as well as $r_\pm$ independently of time. Then to evaluate integral (109) it suffices to know how to evaluate

$$I(a, b, c, d, k) = \int_c^d \frac{r^k dr}{\sqrt{(b-r)(r-a)}} \tag{110}$$

where in all cases, $a, b, c, d \geq 0$ and $c \leq r \leq d$. Specific forms are known for some k. (The integrals are left in indefinite form.)

$$I(a, b, x, -1) = \frac{\arctan\left(\frac{x(a+b)-2ab}{2\sqrt{ab(b-x)(x-a)}}\right)}{\sqrt{ab}} \tag{111}$$

$$I(a, b, x, 0) = \arcsin\left(\frac{2x - b - a}{b - a}\right) \tag{112}$$

$$I(a, b, x, 1) = \frac{a+b}{2}\arcsin\left(\frac{2x - a - b}{b - a}\right) - \frac{b-a}{2}\sqrt{1 - \left(\frac{2x - a - b}{b - a}\right)^2}\,. \tag{113}$$

12. Appendix - Hardware and Software

Mathematica was used for its symbolic manipulation abilities, as well as its built in interval arithmetic. It was used to verify the claims in the technical appendices. It also is used to symbolically differentiate the perturbation term in Delauney and compute the twist term. Furthermore Mathematica's built in numerical integrator allowed us to model results quickly and get estimates on the quantities involved in the action comparison. We made heavy use of the CAPD (Computer Assisted Proofs in Dynamics) library which is written in C++ to perform the rigorous numerical integration. CAPD can be obtained at capd.ii.uj.edu.pl . CAPD is a library which provides objects for intervals, vectors, matrices, maps, and integrators which can be included into C++ programs. CAPD's interval libraries and rigorous integrators were used to perform the action comparison rigorously. The programs written in Mathematica and CAPD can be obtained online at `www.math.umd.edu/ joepi`.

The software ran continuously for two weeks, distributed over a cluster of 15 machines the fastest of which was a 3.4 GHz Pentium 4 with 2GB RAM and 120 GB HDD. It produced over 16GB of data. Each machine was running Linux with latest available build of CAPD and Mathematica 5.0 or better.

Acknowledgements

The first author is particularly grateful to Daniel Wilczak for assistance and advice on the CAPD library. The first author would like to acknowlegde discussions with Martin Berz and Alexander Wittig on rigorous numerics. The first author is grateful to Kory Pennington, Paul Wright, Christian Sykes, and the Mathematics Department at the University of Maryland - College Park for their donation of computer equipment and computer time. The second author would like to acknowledgement discussions with Alain Albouy, Alain Chenciner, Dmitry Dolgopyat, Jacques Fejoz, Rafael de la Llave, and Rick Moeckel. The second author was partially supported by the NSF grant DMS-0701271.

References

[AKN] Arnold, Vladimir I.; Kozlov, Valery V.; Neishtadt, Anatoly. I. Mathematical aspects of classical and celestial mechanics. [Dynamical systems. III]. Translated from the Russian original by E. Khukhro. Third edition. Encyclopaedia of Mathematical Sciences, 3. Springer-Verlag, Berlin, 2006. xiv+518 pp. ISBN: 978-3-540-28246-4; 3-540-28246-7.

[Ban] Bangert, V. Mather sets for twist maps and geodesics on tori. Dynamics reported, vol. 1, 1–56, Dynam. Report. Ser. Dynam. Systems Appl., 1, Wiley, Chichester, 1988.

[Ber] Bernard, Patrick. Symplectic aspects of Mather theory. Duke Math. J. **136(3)** (2007), 401–420.

[BK] Bourgain, Jean, Kaloshin, Vadim. On diffusion in high-dimensional Hamiltonian systems. J. Funct. Anal. **229(1)** (2005),

[BoMa] Bolotin, S.(1-WI); MacKay, R. S. Nonplanar second species periodic and chaotic trajectories for the circular restricted three-body problem. Celestial Mech. Dynam. Astronom. **94(4)** (2006), 433–449.

[CC] Celletti, Alessandra; Chierchia, Luigi. KAM stability and celestial mechanics. Mem. Amer. Math. Soc. **187(878** (2007), viii+134 pp.

[F] Albert Fathi. Weak KAM Theorem in Lagrangian Dynamics. Seventh Preliminary Version.

[D] Chris Davis. Idle theory (1998).

[dLII] de la Llave, Rafael. A tutorial on KAM theory. Smooth ergodic theory and its applications (Seattle, WA, 1999), 175–292, Proc. Sympos. Pure Math., 69, Amer. Math. Soc., Providence, RI, 2001.

[GK2] Galante, J.R., Kaloshin, V. Construction of a Twisting Coordinate System for the Restricted Circular Planar Three Body Problem. Manuscript. Available at `http://www-users.math.umd.edu/ joepi/downloads.html`

[GK3] Galante, J.R., Kaloshin, V. Destruction of Invariant Curves in the Restricted Circular Planar Three Body Problem Using Ordering Condition. Manuscript. Avaliable at `http://www-users.math.umd.edu/ joepi/downloads.html`

[IEEE] IEEE-ANSI. Standard for Binary Floating-Point Arithmetic. 1985.

[J] Jungreis, Irwin. A method for proving that monotone twist maps have no invariant circles. Ergodic Theory Dynam. Systems **11(1)** (1991), 7984.

[K] Kaloshin, Vadim. Geometric proofs of Mather's connecting and accelerating theorems. Topics in dynamics and ergodic theory, 81–106, London Math. Soc. Lecture Note Ser., 310, Cambridge Univ. Press, Cambridge, 2003.

[KN] V. Kaloshin, T. Nguyen. Remote Periodic and Quasiperiodic Motions in the Planar Circular Restricted 3-Body Problem of KAM and Aubry-Mather Type. Preprint.

[KNP] V. Kaloshin, T. Nguyen, D. Pavlov. Nonlocal Instabilities of the Restricted Planar Circular Three Body Problem. Manuscript.

[KM] Kulisch, Ulrich W.; Miranker, Willard L. Computer arithmetic in theory and practice. Computer Science and Applied Mathematics. Academic Press, Inc. [Harcourt Brace Jovanovich, Publishers], New York-London, 1981. xv+249 pp. ISBN: 0-12-428650-X

[LS] Llibre, Jaume; Simo, Carlos. Oscillatory solutions in the planar restricted three-body problem. Math. Ann. **248(2)** (1980), 153–184.

[Ma] Mather, John N. Variational construction of connecting orbits. Ann. Inst. Fourier (Grenoble) **43(5)** (1993), 1349–1386.

[MF] Mather, John N.; Forni, Giovanni Action minimizing orbits in Hamiltonian systems. Transition to chaos in classical and quantum mechanics (Montecatini Terme, 1991), 92–186, Lecture Notes in Math., 1589, Springer, Berlin, 1994.

[McG] McGehee, Richard A stable manifold theorem for degenerate fixed points with applications to celestial mechanics. J. Differential Equations **14** (1973), 70–88.

[Mo1] J. Moser. Recent Development in the Theory of Hamiltonian Systems. SIAM Review, **28(4)** (1986), 459–485.

[Mo2] J. Moser. Monotone twist mappings and the calculus of variation. Ergodic Theory and Dynamical Systems **6** (1986), 401–413.

[MZ] Mrozek, Marian; Zgliczynski, Piotr. Set arithmetic and the enclosing problem in dynamics. Dedicated to the memory of Bogdan Ziemian. Ann. Polon. Math. **74** (2000), 237–259.

[PB] Petrosky, T. Y.(1-TX-I); Broucke, R. Area-preserving mappings and deterministic chaos for nearly parabolic motions. Celestial Mech. **42(1-4)** (1987/88), 53–79.

[S] Siburg, Karl Friedrich. The principle of least action in geometry and dynamics. Lecture Notes in Mathematics, 1844. Springer-Verlag, Berlin, 2004. xii+128 pp. ISBN: 3-540-21944-7

[WZ] D. Wilczak, P. Zgliczynski, The C^r Lohner-algorithm. Preprint.

[X] J. Xia, Arnold Diffusion and Instabilities in Hamiltonian Dynamics. Preprint.

[Z] Zgliczynski, Piotr. C^1 Lohner algorithm. Found. Comput. Math. **2(4)** (2002), 429–465

Joseph Galante
Department of Mathematics
Mathematics Building
University of Maryland
College Park, MD 20742-4015, USA
E-mail address: joepi@math.umd.edu

Vadim Kaloshin
Department of Mathematics
Mathematics Building
University of Maryland
College Park, MD 20742-4015, USA
E-mail address: kaloshin@math.umd.edu